

# **Role of DVE-1 and higher chromatin organization in ageing of *Caenorhabditis elegans***

A Thesis

submitted to

Indian Institute of Science Education and Research Pune in partial fulfilment of the requirements for the BS-MS Dual Degree Programme

by

Keshav Jha

20151111



Indian Institute of Science Education and Research Pune

Dr. Homi Bhabha Road,

Pashan, Pune 411008, INDIA.

April, 2020

Supervisor: Prof Sanjeev Galande

## Certificate

This is to certify that this dissertation entitled 'Role of DVE-1 and higher chromatin organization in the ageing of *Caenorhabditis elegans*' towards the partial fulfilment of the BS-MS dual degree programme at the Indian Institute of Science Education and Research, Pune represents study/work carried out by Keshav Jha at Indian Institute of Science Education and Research under the supervision of Prof. Sanjeev Galande, Department of Biology, during the academic year 2019-20.

Handwritten signature of Keshav Jha in blue ink, underlined.

Keshav Jha

3<sup>rd</sup> April 2020

Handwritten signature of Prof. Sanjeev Galande in black ink, underlined.

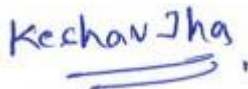
Prof. Sanjeev Galande

Supervisor

This thesis is dedicated to my dearest Grandpa

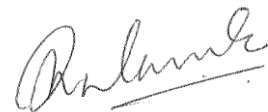
## Declaration

I hereby declare that the matter embodied in the report entitled 'Role of DVE-1 and higher chromatin organization in the ageing of *Caenorhabditis elegans*' is the results of the work carried out by me at the Department of Biology, Indian Institute of Science Education and Research, Pune, under the supervision of Prof. Sanjeev Galande and the same has not been submitted elsewhere for any other degree.

Handwritten signature of Keshav Jha in blue ink, with a horizontal line underneath.

Keshav Jha

3<sup>rd</sup> April 2020

Handwritten signature of Prof. Sanjeev Galande in black ink, with a horizontal line underneath.

Prof. Sanjeev Galande

Supervisor

## Acknowledgments

I would like to foremost thank my thesis supervisor, Prof. Sanjeev Galande to allow me to work alongside in his lab and for being a constant source of guidance and encouragement throughout this project. I would also to thank Dr. Sneha Sagarkar for her scientific and technical inputs in the planning and execution of the experiments.

I am thankful to the expert member of my TAC, Dr. Kavita Babu of IISc, Bangalore for her valuable time and guidance during the project. Her suggestions were extremely beneficial. Thanks to our project collaborator, Dr. Arnab Mukhopadhyay of NII, New Delhi for providing us with the essential reagents and training me for micro-injection and construction of transgenic strains of worms. I would also like to acknowledge Dr. G P Manjunath of NYU Langone Medical Center for his valuable previous work on this project.

I find myself extremely lucky to have worked next to such talented and amiable members of SG and KK lab. I wish to thank Sourabh Pradhan, Ankita Sharma, and Amit Karole for their valuable inputs in various experiments of this project. A special thanks to Mukul Ravat and Abhishek Kanyal of KK Lab for their support and selfless help as friends and seniors. Finally, I would like to thank the Department of Biology, IISER Pune to extend all the state-of-the-art facilities available in the institute.

# List of Contents

Abstract.....	10
Chapter 1 .....	11
1.1 Ageing.....	12
1.2 Popular theories of ageing.....	14
1.2.1 Programmed theory of ageing.....	14
1.2.2 Damage theory .....	15
1.3 Gerontology.....	16
1.4 <i>Caenorhabditis elegans</i> as a model to study organismal ageing.....	17
1.4.1 Lifecycle of <i>C. elegans</i> .....	17
1.5 Pathways associated with Lifespan in <i>C. elegans</i> .....	19
1.5.1 Insulin/IGF-1 Signaling.....	19
1.5.2 Unfolded Protein Responses and longevity .....	19
1.6 <i>Defective proventriculus (dve)</i> .....	22
Chapter 2.....	23
2.1 Culture and Maintenance of <i>Caenorhabditis elegans</i> .....	24
2.1.1 Worm Strains .....	24
2.1.2 Growth Media.....	25
2.1.3 Bacterial Strains.....	27
2.2 Phenotypic Assays .....	27
2.2.1 Lifespan Assay.....	27
2.2.2 Temperature stress assay.....	28
2.2.3 Oxidative stress assay .....	28
2.3 Molecular Biology .....	28
2.3.1 DNA extraction and genotyping.....	28
2.3.2 Worm Lysis and total protein extraction.....	29
2.3.3 Immunoprecipitation (IP) and Western blotting.....	29
2.3.3 Nuclear Cytoplasmic Fractionation.....	30
2.3.4 Chromatin Immunoprecipitation (ChIP) .....	30
2.3.5 RNA Isolation from worms.....	31
2.3.6 DNase treatment of isolated RNA .....	32

2.3.7 cDNA synthesis.....	32
2.3.8 Real-time PCR .....	32
2.3.9 Antibodies .....	33
2.3.10 Primers .....	34
Chapter 3.....	35
3.1 Introduction.....	36
3.2 Results .....	36
3.2.1 DVE-1 and DAF-16 have common genomic targets .....	36
3.2.2 Validation of monoclonal antibody raised against DVE-1.....	38
3.2.4 DAF-16 co-immunoprecipitates with DVE-1 and vice-versa .....	39
3.2.5 Confirmation of the interaction of DVE-1 and DAF-16 on the chromatin .....	41
3.3 Discussion and future directions .....	43
Chapter 4.....	45
4.1 Introduction.....	46
4.2 Results .....	46
4.2.1 <i>dve-1<sup>tm4803</sup></i> confers longevity and higher stress tolerance to <i>C. elegans</i> .....	46
4.2.2 Phenotypic characterization of <i>dve-1<sup>tm4803</sup></i> worms .....	48
4.2.3 <i>dve-1<sup>tm4803</sup></i> don't form dauer at the non-permissive temperature .....	50
4.2.4 Effect of <i>dve-1</i> RNAi on stress resilience of worms .....	51
4.2.5 Transcriptome analysis of <i>dve-1<sup>tm4803</sup></i> reveals differential gene expression in multiple pathways .....	52
4.2.6 GO-term analysis of upregulated genes explained the thermal resilience of <i>dve-1<sup>tm4803</sup></i> .....	53
4.3 Discussion and future directions .....	54
References .....	57
Appendix: Raw data for phenotypic assays.....	65

# List of Figures and Tables

## Chapter 1

Figure 1. 1. Statistics of increased human life expectancy and age onset of diseases.....	13
Figure 1. 2. WormAtlas: Life cycle of <i>C. elegans</i> .....	18
Figure 1. 3. Domains of huSATB1 and CeDVE-1 .....	22

## Chapter 3

Figure 3. 1. DVE-1 and DAF-16 share common targets on the genomic loci.....	37
Figure 3. 2. Confirmation of the specificity of the home-raised monoclonal antibody.....	38
Figure 3. 3. DVE-1 and DAF-16 interact with each other.....	40
Figure 3. 4. Effect of temperature stress on the localization of DVE-1 and DAF-16.....	40
Figure 3. 5. Optimization of sonication for the shearing of the chromatin from worms .....	41
Figure 3. 6. Enrichment of DVE-1 and DAF-16 on the promoters of <i>hsp-6</i> and <i>hsp-60</i> .....	42
Figure 3. 7. DAF-16 co-immunoprecipitated with DVE-1 after Chromatin immunoprecipitation.....	43

## Chapter 4

Figure 4. 1. <i>dve-1<sup>tm4803</sup></i> has homozygous deletion in <i>dve-1</i> gene.....	47
Figure 4. 2. Domain architecture of DVE-1 <sup>WT</sup> vs DVE-1 <sup>tm4803</sup> .....	47
Figure 4. 3. Lifespan assay of <i>dve-1<sup>tm4803</sup></i> and N2.....	48
Figure 4. 4. Oxidative and thermal stress assay of worms .....	49
Figure 4. 5. Dauer formation assay .....	50
Figure 4. 6. Stress assay upon knockdown of <i>dve-1</i> .....	51
Figure 4. 7. Volcano plot of the differentially-regulated genes .....	52
Figure 4. 8. GO-term analysis of differentially expressed genes.....	53
Figure 4. 9. GO-term analysis of upregulated genes .....	54
Figure 4. 10. Expression level of chaperones of different sub-cellular compartment .....	54
Table 1. Lifespan assay of N2 and <i>dve-1<sup>tm4803</sup></i> .....	65
Table 2. Temperature stress assay .....	65
Table 3. TBHP stress assay.....	65
Table 4. Dauer formation assay .....	66



## List of Abbreviations

ABC	ATP-binding cassette
BCA	Bicinchoninic acid
cDNA	complementary DNA
CR	Caloric restriction
Ct	Cycle threshold
DAF	Dauer formation
ChIP	Chromatin immunoprecipitation
DNA	Deoxyribonucleic acid
DVE	Defective proventriculus
ER	Endoplasmic reticulum
FC	Fold change
FTT	Fourteen-Three-Three
GFP	Green fluorescent protein
GO	Gene ontology
HSP	Heat shock protein
IGF-1	Insulin-like growth factor-1
IgG	Immunoglobulin G
ILP	Insulin-like peptides
IRE	Insulin responsive elements
KD	Knockdown
mt	Mitochondria
PCR	Polymerase chain reaction
PIC	Protease inhibitory cocktail
PVDF	Polyvinilidene fluoride
qRT-PCR	Quantitative real-time PCR
RNA	Ribonucleic acid
RNAi	RNA interference
ROS	Reactive oxygen species
RT	Room temperature
SATB1/SATB2	Special AT-rich binding protein1/2
TBHP	tert-Butyl hydroperoxide
TES	Transcription end site
TSS	Transcription start site
UPR	Unfolded protein response

## Abstract

The competency of an organism to sense the stressful conditions and appropriately respond to them determines its survivability. Insulin/IGF-1 signaling is one of the most studied pathways that sense different stress conditions and its downstream effector, DAF-16/FOXO modulates the expression level of various stress-responsive and pro-longevity genes. However, the ability of this pathway to suffice for the necessary transcriptional changes in diverse stress conditions remains elusive. In the first study, using *C. elegans* as the model system we for the first time show that DAF-16 forms complex with a homeobox transcription factor, DVE-1 and binds to the promoters of a large number of longevity genes. This complex formation may have a combinatorial effect in setting different transcriptional paradigms appropriate for the survival of organisms in different stress conditions. In a separate study, we investigated a mutation in *dve-1* gene that conferred longevity and exceptional stress-responsive capabilities to the worms. Using high-throughput experiments and additional biochemical techniques, we dissected out the mechanisms that led to these observed phenotypes in the mutant worms. These findings strengthen our understanding of how various transcription factors act as a part of a transcription module that senses the stressful conditions and establishes global gene expression patterns to mitigate stress and promote longevity.

# Chapter 1

## Introduction

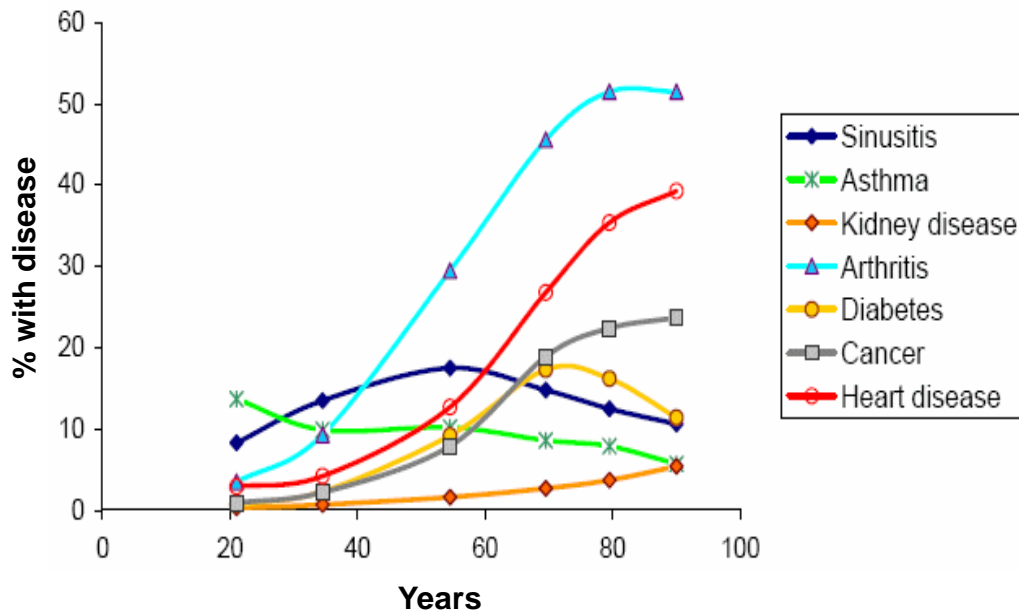
## 1.1 Ageing

Typically, an organism during its lifetime goes through the maturation phase followed by the reproductive phase and finally with progressive deterioration of the health becomes aged and dies eventually. Ageing has been believed to be an inevitable process that ultimately ends with the demise of the organism. It is usually associated with the loss of general health and the occurrence of physical and mental ailments. Along with the degradation of the skin, muscle, nerves and the general bodily homeostasis, many diseases like cancer, cardiovascular diseases, diabetes, arthritis, etc. arise more frequently in the aged human (Fig. 1A). Also, in the recent outbreak of COVID-19, the maximum mortality rate was observed in the individual of the older age group with compromised immunity (WHO, Situation report- 46).

The average age of the human population has been increasing and is highest than ever before. The reason for this is the increased life expectancy which surged from the world average of 32 years in 1900 to 72 years in 2018 (Fig.1B). In developing countries like India, the life expectancy which was mere 36 years during the time of its independence in 1947 increased to nearly 69 years by 2019. This increase in life expectancy can be attributed to modern health care advancements and overall geopolitical stability.

Ageing research in the last few decades has been focused on finding new pathways of ageing in the lower model systems and drawing insights from them to understand human ageing. Recent studies have also involved higher model systems like flies, mice and also primates like rhesus monkeys to test drugs that extended lifespan (Francisco and Ranch, 1998). There have been several longitudinal studies on human subjects in which the health of the same individual had been tracked throughout the life (Maras et al., 2011; Austad, S. 1999). Coupled with the advancement in molecular biology and new bioinformatics tools, this would potentially open new windows to understanding the complexity of human ageing and novel therapeutic approaches to curb the age-associated diseases. Rapamycin, resveratrol, metformin, etc. are some of the successful anti-ageing drugs which have been discovered and tested.

A)



B)

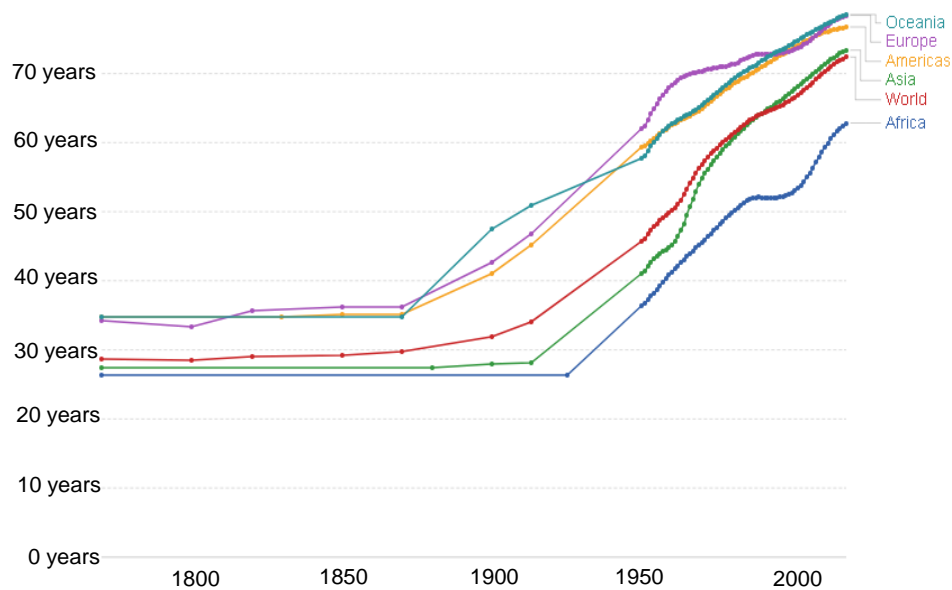


**Figure 1. 1. Statistics of increased human life expectancy and age onset of diseases.**

A) Prevalence of diseases like cancer, arithritis, asthma, kidney diseases etc. in US population become more frequent after the age of 60 years (2002-2003) (Source: National Centre for Health Statistics, Data Warehouse on Trends in Health and Ageing) B) World average life expectancy raised from 30 years in 1800 to over 70 years in 2000. (data from OurWorldInData.org/life-expectancy)

## **1.2 Popular theories of ageing**

Why do living beings age? When does ageing onsets and are there general markers of ageing? Over the years there have been many attempts to answer these questions but to date, there has been no single theory to explain them all. The popular theories of ageing can be generally classified into two groups, programmed theory and damage theory of ageing.

### **1.2.1 Programmed theory of ageing**

According to this theory, ageing is akin to other stages of life like childhood or adulthood. These stages are the consequences of the hard-wired gene regulatory networks that govern the gene expression pattern at every stage of life including the one that leads to the ageing phenotypes during the old age (Davidovic et al., 2010). This theory can be further divided into sub-categories like Endocrine theory, Immunological senescence theory, etc.

#### **1.2.1.1 Endocrine Signaling theory**

From the physiological studies, it is well known that hormones play an important role in developmental process growth and ageing. For instance, Insulin and IGF-1 signaling have been one of the most studied pathways that dictate the stress response and rate of ageing (van Heemst, 2010).

#### **1.2.1.2 Immunological senescence theory**

Throughout the lifetime, the immune system of the organism weakens and loses the ability to defend itself from infections (Cornelius, 1972). Immunosenescence is one of the key features during the ageing in mammals accompanied by blood ageing

phenotypes and higher risk of hematological cancers (Hassan and Abedi-Valugerdi, 2014; Zweegman et al., 2014).

### **1.2.2 Damage theory**

This theory bases ageing to be an outcome of the insult faced by the organism due to the surrounding environment or by damage-causing agents within itself. There have been several theories that have been put forward on this basis.

#### **1.2.2.1 Wear and tear theory**

This theory was proposed by the German evolutionary biologist, August Weismann in 1882. It states that the organisms accumulate wear and tear in their lifetime which leads to ageing and eventual death(Kirkwood and Cremer, 1982). This is one of the widely accepted theories of ageing until today.

#### **1.2.2.2 Free Radical theory**

This was proposed by Prof. Rebeca Gerschman in 1951(Gerschman et al., 1954). Free radicals and superoxides are byproducts of the metabolic process in the cell and cause damage to the macromolecules like proteins, sugars, and nucleic acids. In the DNA, these molecules can lead to single-nucleotide mutations and even double-strand breaks. These damages gradually result in the loss of cellular homeostasis and have been known to be the cause for the onset of many age-related pathologies like Alzheimer's, Parkinson's disease, cancer, etc.(Drechsel and Patel, 2008; Gredilla and Barja, 2005; Liou and Storz, 2010) Reactive oxygen species (ROS) are one of the most commonly formed free radicals during the oxidative phosphorylation in the mitochondria. Cells have evolved ROS scavengers as a mechanism to keep them in control (Sharma et al., 2012).

### **1.2.2.3 Telomere shortening theory**

American anatomist, Leonard Hayflick in 1961 demonstrated that human fetal cells maintained ex-vivo in tissue culture underwent senescence after 40-60 passages (Hayflick, 1965). Hayflick's limit is defined to be the number of cycles of division that a cell type undergoes before it starts to show the signs of senescence and stop dividing (Ruben and Biology, 2000). This concept disproved the earlier notion of the immortality of human cell explants maintained in tissue culture.

Telomeres are the regions at the end of the chromosomes with repetitive nucleotide sequences that protect the loss of nucleotides during replication. Telomerase act to attach extra repetitive sequences to compensate for this loss after every replication cycle. The dividing cells usually are devoid of this machinery and undergo senescence after the hayflick's limit (Ruben and Biology, 2000). The stem cells over time lose pluripotency due to the inability of telomere regeneration (Hiyama and Hiyama, 2007).

### **1.3 Gerontology**

Gerontology is the scientific study of ageing and the pathologies associated with it. The field started with the experiments by Clive McCay and Mary Crowell related to caloric restrictions (CR) in the mouse which not only delayed ageing but also kept the animals healthy for longer periods (McCay et al., 1935). A similar effect of CR has been observed in other model systems like *Drosophila* and *C. elegans* (Chapman and Partridge, 1996; Klass, 1977). The modern gerontology aims to study the ageing process using genetic manipulations in the model systems coupled with the molecular biology techniques and bioinformatics analysis to dissect out pathways associated with it.



## 1.4 *Caenorhabditis elegans* as a model to study organismal ageing

Studying the molecular mechanism of ageing had been particularly challenging because of the longer lifespan of the commonly used model systems. *Caenorhabditis elegans* are 1mm long nematodes with a lifespan of 2-3 weeks, ideal for the ageing experiments. In addition to it, worms offer the relative ease of maintenance of culture and offer robust genetic manipulations. The genetic resources available for worms include the whole genome RNA interference (RNAi) library (Ceron et al., 2004; Kamath and Ahringer, 2003) enabling genome-wide RNAi screens, hundreds of publicly available mutants and over 2000 promoter::GFP constructs. The high throughput sequencing and analysis are feasible with the entire genome sequenced and well-annotated (Harris et al., 2004; Räscht et al., 2007).

*C. elegans* like mammals show signs of ageing and age-related degeneration of health. It has been extensively used as the model to study the pathologies due to the loss of proteostasis in neurodegenerative diseases like the accumulation of amyloid-beta in Alzheimer's disease (Link, 1995), Poly-Q in Parkinson's disease (Lakso et al., 2003) and Huntington's disease (Faber et al., 1999). Besides, worms have been used for identifying the therapeutic targets of these diseases and also screening drugs to ameliorate these pathologies (Ikenaka et al., 2019; O'Reilly et al., 2014).

### 1.4.1 Lifecycle of *C. elegans*

*C. elegans* under the optimal nutrient condition has an average lifespan of 2-3 weeks in which they hatch from the egg, go through the four larval stages to become adults, grow old and die. A wildtype adult worm can lay up to 250 to 300 eggs with self-fertilization (Muschiol et al., 2009). These eggs are internally fertilized in the body of the mother and are laid out with the beginning of the formation of the germ layers in the 30-celled stage. Further, the embryos undergo extensive cell proliferation and cell migration for the organogenesis. Embryonic development lasts approximately 14 hours with the formation of the L1 larva (Sulston et al., 1983). In the absence of food, L1s do not proceed further in development and live up to a week. When grown in the nutrient-rich medium, the L1 larvae increase in size to enter the second larval stage

L2. The vulval development begins in the third larval stage, L3 and completes by the end of the fourth stage, L4 (Antebi et al., 1997). An adult worm lays fertilized eggs up to 4 days of its adulthood after which it enters the post-reproductive life. The worms continue to grow in size, accumulate fat bodies and live up to 10-15 more days.

There is another developmental checkpoint that exists between the L1 and L2 stage. The worms in the nutritional stress or overcrowding in the surrounding, stall their reproductive development and enter a highly stress-resistant and long-lived diapause state called dauers (Riddle, 1988; Gottlieb and Ruvkun, 1994). With stopped feeding, dauers look slender in shape with thickened cuticles. Once the worms sense the availability of food again, they exit the diapause state and continue with the normal development to directly enter in L4 stage (Cassada and Russel, 1975).

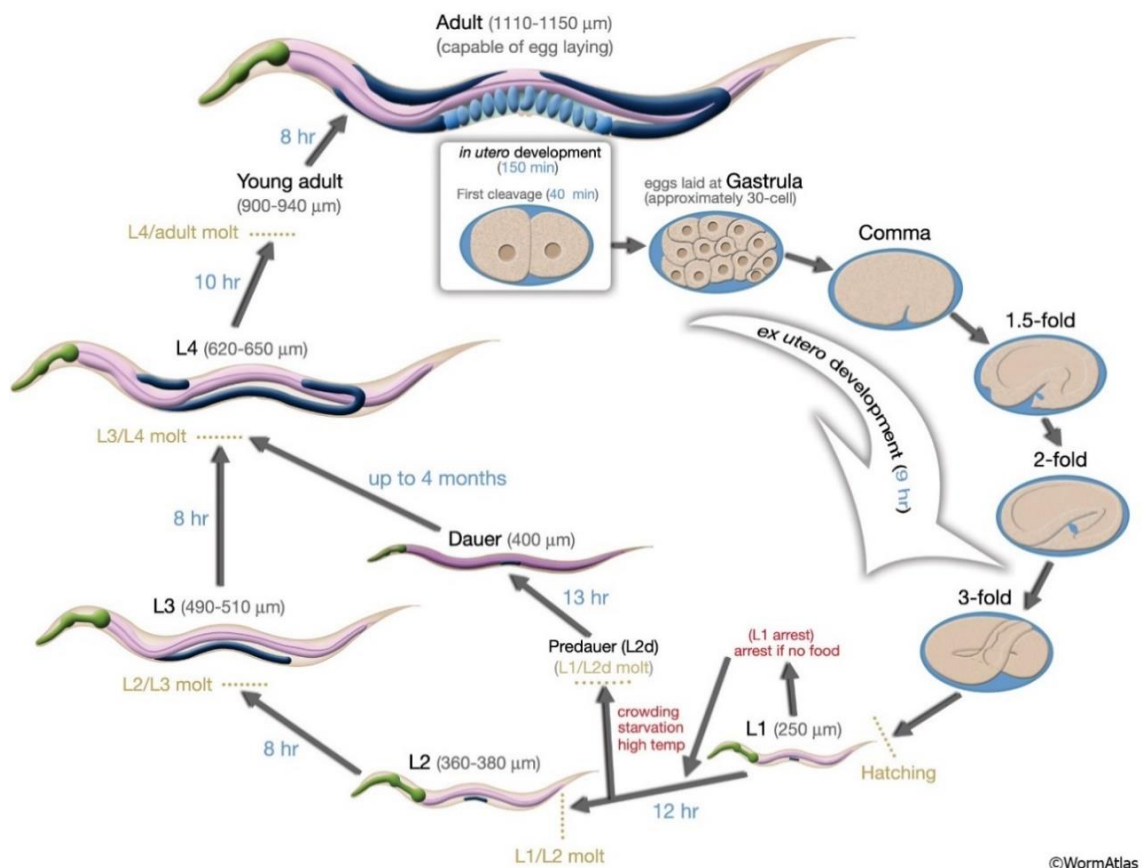


**Figure 1. 2. WormAtlas: Life cycle of *C. elegans*.**

The life cycle of worm has four larval stages after which the worm becomes a reproductive adult. Pheromones, lack of food or over-crowding can trigger the dauer formation after the L1 stage (Reproduced from the WormAtlas).

## **1.5 Pathways associated with Lifespan in *C. elegans***

### **1.5.1 Insulin/IGF-1 Signaling**

Insulin/ IGF-1 signaling is a highly conserved pathway and has been extensively studied for its role in stress response and longevity. *C. elegans* have over 40 Insulin-like peptides (ILPs) that are secreted from the sensory neurons when the worms sense the availability of food in the vicinity (Pierce et al., 2001). These ILPs bind to the Insulin receptor, Abnormal Dauer Formation-2 (DAF-2) in the intestine, leading to the autophosphorylation and activation of its intrinsic tyrosine activity (Luo et al., 1999). The activated DAF-2 phosphorylates phosphoinositide-3-kinase (PI3K) which leads to the accumulation of 3-phosphoinositide (PIP<sub>3</sub>) in the cell membrane (Cantrell, 2001). Kinase, AKT-1 is recruited by PI3K and gets phosphorylated at two conserved residues. Phosphorylated AKT then phosphorylates DAF-16 which in turn is retained in the cytoplasm by two 14-3-3 proteins, Fourteen-Three-Three (FTT-2) and PAR-5 (FTT-1) (Berdichevsky et al., 2006). In the absence of Insulin signaling, this kinase pathway remains inactive and DAF-16 undergoes nuclear localization to bind on to its target genes. DAF-16 upregulates genes that are responsible for dauer formation, stress response, fat storage and overall longevity (Kimura et al. 1997).

### **1.5.2 Unfolded Protein Responses and longevity**

Cellular proteins are susceptible to misfolding and lose their functional property. If unchecked, these misfolded proteins can aggravate ageing and related pathologies. Cells have evolved mechanisms to ensure the stringent quality control of proteins and maintain proteostasis. The misfolded proteins are either folded again by the chaperones or degraded by proteolytic enzymes. The Unfolded protein responses (UPRs) are conserved stress responsive signaling pathways to counter the accumulation of unfolded proteins in the subcellular compartments (Bertolotti et al., 2000). UPRs are usually specific to every compartment, upregulating the expression of organelle-specific chaperones or proteolytic machinery for the effective mitigation of stressors (Pellegrino et al., 2013).

### 1.5.2.1 Cytoplasmic Unfolded Protein Response

In a typical cell, proteins make up 20-30% of the cytosol (Ellis, 2001). With a relatively lesser degree of post-translational modifications, these proteins are most susceptible to temperature-associated misfolding. The misfolding is sensed by the cytosol-resident chaperones like hsp-70 and hsp-90 (Pratt and Toft, 2003). These chaperones interact with stretches of hydrophobic residues of the proteins which are usually deeply buried in the tertiary structures of the proteins in the folded state (Mayer and Bukau, 2005). These chaperones can refold the unfolded proteins in an ATP-dependent fashion.

The *hsp-16* (*hsp-16.11*, *hsp-16.2*, *hsp-16.48*) family of chaperons in *C. elegans* are primary effectors of cytoplasmic UPR. Under the heat stress, HSF-1 undergoes nuclear localization and bind to the promoters of these genes and upregulate their expression. (Hsu et al., 2003). This quality control system is critical for the lifespan of the organisms as *hsf-1* KO animals show increased aggregation of poly-Q and are short-lived (Cohen et al., 2010).

### 1.5.2.2 Endoplasmic Reticulum specific Unfolded Protein Response

Proteins in ER are susceptible to errors in post-translational modifications like membrane insertion, glycosylation, the formation of disulfide bonds, etc. But due to these modifications, these proteins are resilient to temperature stress. There are three known pathways through which UPR<sup>ER</sup> is mediated. The first pathway involves the ribonuclease, Inositol Requiring Protein-1 (IRE-1) which upon ER stress cleaves an intron in the mRNA of X-box Binding Protein-1 (XBP-1) to form the activated form of XBP-1. XBP-1 upregulated the expression level of ER-resident chaperone, HSP-4 for the refolding of the proteins and the components of ER-associated degradation (ERAD) for degradation (Scheuner et al., 2001). The second pathway involves the Serine/Threonine kinase, PEK-1 which under ER stress phosphorylate ELF-2, in turn inhibiting the assembly of 80s ribosomal subunit to decrease the global translation and protein folding load on ER (Shi. Y et al., 1998). The third pathway is through the transcription factor, ATF-6 which normally localizes in the ER membrane but

translocates to Golgi where it gets activated by the Golgi resident proteases and further activates genes to mitigate the ER stress (Shen et al., 2001).

### **1.5.2.3 Mitochondrial Unfolded Protein Response**

Mitochondria are the powerhouses for the cells, generating ATPs via oxidative phosphorylation, essential for the maintenance of the cellular processes. Mitochondrial proteins are partially coded by the mitochondrial DNA and rest by nuclear DNA (Mishra and Chan, 2014). Mutations in these genes can cause mitochondrial dysfunction leading to increased production of ROS, damaging the organelles. This is accelerated during ageing and exacerbates the pathologies associated with neurodegeneration in Alzheimer's and Parkinson's disease (Keane et al., 2011; Moreira et al., 2010).

Mitochondrial unfolded protein response (UPR<sup>mt</sup>) is the protective response by the cells to ameliorate the mitochondrial damage. It starts with the accumulation of unfolded proteins in the mitochondrial matrix. The matrix protease, CLPP-1 cleaves these unfolded proteins into stretches of small peptides which are then transported out into the cytoplasm by an ABC transporter, HAF-1 (Haynes et al., 2007). This is thought to weaken the import machinery of mitochondria. Transcription factor, ATFS-1 which has both nuclear and mitochondrial localization signals is typically transported into the mitochondria and degraded by LON protease. In mitochondrial stress, ATFS-1 accumulates in the cytoplasm and then translocates to the nucleus and initiates the protective transcriptional regime (Nargund et al., 2012). DVE-1, the SATB1 homolog in *C. elegans* along with its binding partner, UBL-5 also translocates to the nucleus and binds to the promoters of mitochondrial chaperones and increases their expression (Haynes et al., 2007).

## 1.6 Defective proventriculus (*dve*)

The homolog of SATB1, DVE was found to be a transcriptional repressor in *Drosophila melanogaster* and essential for various functions like ommatidial and midgut specification, male accessory organ development, etc. (Johnston et al., 2011; Nakagawa et al., 2011; Haynes et al., 2007; Minami et al., 2012). The homolog in *C. elegans*, DVE-1 was found in an RNAi screen to identify the genes which upon KD didn't activate UPR<sup>mt</sup> (Haynes et al., 2007).

DVE-1 is a 468aa protein that has 34% sequence identity with huSATB1. It contains N-terminal PDZ-domain to interact with other transcription factors and two homeobox domains to facilitate DNA binding. There are two other predicted isoforms which are smaller in size and harbor only either of the domains (Fig. 1.3). Besides, DVE-1 is known to be SUMOylated at the K327 residue which governs its nuclear-cytoplasmic localization. SUMOylated DVE-1 is rendered in cytoplasm while under mitochondrial stress this modification is cleaved by ULP-4 and it accumulates in the nucleus (Gao et al., 2019).

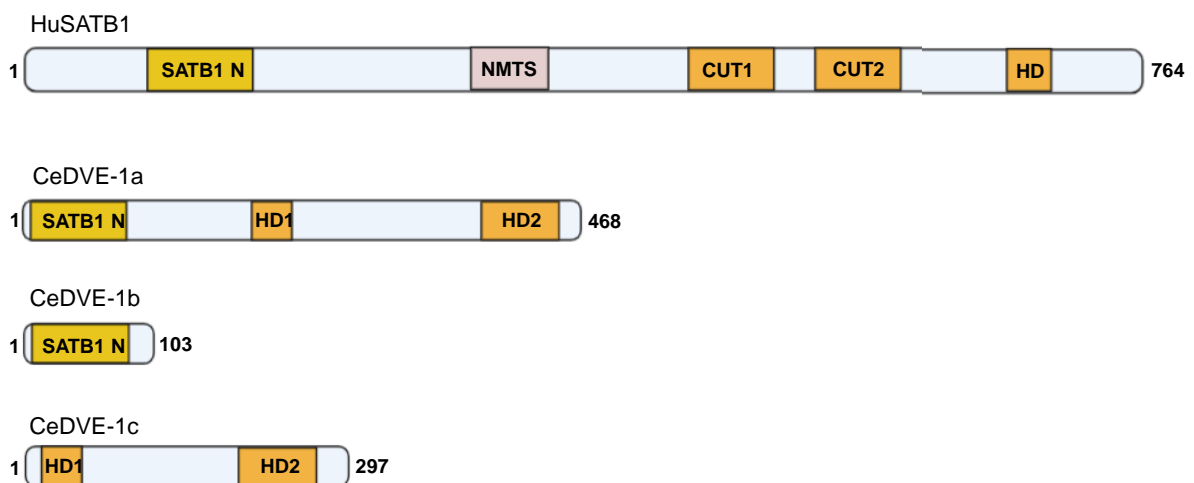


**Figure 1. 3. Domains of huSATB1 and CeDVE-1.**

Human SATB1 harbors an N-terminal ULD domain, nuclear matrix-binding domain (NMTS), and the CUT and homeobox domains for binding to DNA. The largest isoform of DVE-1 contains the SATB1 N-terminal domain and two homeobox domains.

# Chapter 2

## Materials and Methods

## 2.1 Culture and Maintenance of *Caenorhabditis elegans*

### 2.1.1 Worm Strains

All the worms used in this project have been procured from Caenorhabditis Genetics Center (CGC) at the University of Minnesota, USA, and National BioResource Project (NBRP), Japan. We have used the following five strains of worms extensively in the project depending on the type of experiment:

#### **N2 Bristol**

This strain of worms has been used as the control strain for most of the experiments unless specified.

#### ***dve-1<sup>tm4803</sup>***

This strain was procured from NBRP, Japan. The strain harbors a homozygous 509 bp deletion in the ZK1993.5 sequence (*dve-1* gene) but is viable and fertile.

#### **CB1370: *daf-2 (e1370)***

The strain has a point mutation in the *daf-2* gene and leads to a temperature-sensitive constitutive dauer phenotype. The worms form 15% dauers at 20°C and 100% dauers at 25°C.

#### **GR1307: *daf-16 (mgDF50)***

The strain has a complete deletion of the entire CDS of *daf-16*. The worms are short-lived and are dauer defective.

#### **TJ356: *zls356 (daf-16p::*daf-16a/b>::gfp + rol-6)****

The strain has CDS of *daf-16a/b>::gfp* under the control of endogenous promoter, stably inserted in the genome. *rol-6*, the co-injection marker confers the rolling phenotype to the worms. The worms are slightly long-lived and form dauer at 25°C.



## 2.1.2 Growth Media

### 2.1.2.1 Nematode Growth Media (NGM) Lite:

The *Caenorhabditis elegans* were normally grown on the NGM lite medium for the general maintenance of the stock. For 1 l of NGM, 20 g of bacteriological agar, 4 g of peptone, 6 g of NaCl, 9 g of  $\text{KH}_2\text{PO}_4$  and 50 mg of  $\text{K}_2\text{HPO}_4$  was mixed with 980 ml of distilled water and autoclaved. Upon cooling till  $55^\circ\text{C}$ , 4 ml of Cholesterol (2 mg/ml in 100% ethanol) was added and mixed vigorously. The media was then aseptically poured in 100 mm, 60 mm or 30 mm plates and allowed to air-dry overnight. Overnight grown culture of *E. coli* OP50 was spread on the plate and allowed to dry for 16 hours at RT. After the incubation, the bacteria were killed by irradiating with UV for 10 min at full power. The plates were either used to culture worms immediately or stored at  $4^\circ\text{C}$  for later use.

### 2.1.2.2 S-medium

**S-basal:** For 1 L of S-basal, 5.85 g of NaCl, 1 g of  $\text{K}_2\text{HPO}_4$ , 6 g of  $\text{KH}_2\text{PO}_4$  and 1 ml of Cholesterol (5 mg/ml in 100% ethanol) was dissolved in distilled water to make up the volume and autoclaved.

Potassium Citrate: For 1 M Potassium Citrate, 20 g of citric acid monohydrate and 293.5 g of tri-potassium citrate was dissolved in 1 l of distilled water and autoclaved.

Trace metal solution: For 1 L of trace metal solution, 1.86 g of disodium EDTA, 0.69 g of  $\text{FeSO}_4 \cdot 7\text{H}_2\text{O}$ , 0.2 g of  $\text{MnCl}_2 \cdot 4\text{H}_2\text{O}$ , 0.29 g of  $\text{ZnSO}_4 \cdot 7\text{H}_2\text{O}$  and 0.2 g of  $\text{CuSO}_4 \cdot 5\text{H}_2\text{O}$  was dissolved in distilled water to 1 L and autoclaved.

1 M  $\text{CaCl}_2$

55.5 g of  $\text{CaCl}_2$  powder was dissolved in distilled water to make the volume up to 1 L and autoclaved.

1 M MgCl<sub>2</sub>

95.2 g of MgCl<sub>2</sub> powder was dissolved in distilled water to make the volume up to 1 L and autoclaved.

### **S-medium**

For 1 L of S-medium, 974 ml of S-basal, 10 ml of 1M potassium citrate, 10 ml of trace metal solution, 3 ml of 1 M CaCl<sub>2</sub>, 3 ml of 1 M MgSO<sub>4</sub> and 4 ml of Cholesterol (2 mg/ml in 100% ethanol) was mixed. The volume and concentration of E. coli OP50 were added based on the number of worms to be grown.

#### **2.1.2.3 Luria Bertani Broth**

For 1 L of Luria Bertani (LB) broth, 25 g of the LB powder (Himedia, Cat No.: M1245) was dissolved in distilled water to make up the volume. The media was then autoclaved and used to grow the bacterial culture.

#### **2.1.2.4 M9 Buffer**

For 1 L of M9 buffer, 3 g of KH<sub>2</sub>PO<sub>4</sub>, 6 g of Na<sub>2</sub>HPO<sub>4</sub>, 5 g of NaCl, 1 ml of 1 M of MgSO<sub>4</sub> was dissolved in distilled water to make up the volume and autoclaved.

#### **2.1.2.5 Media for the RNAi experiments**

The HT115 bacteria transformed with the dsRNA expressing plasmid is cultured on the Luria Bertani Agar (LA) plates with 12 µg/ml tetracycline (Himedia, CMS219) and 50 µg/ml carbenicillin (Himedia, SD004). The liquid culture for the bacteria was grown in LB with 100 µg/ml carbenicillin.

#### **2.1.2.6 FUdR plate for lifespan assay**

FUdR (Sigma Aldrich Cat No. F0503) was used to inhibit the hatching of eggs to prevent the mixing of mother worms with the progenies in the lifespan experiments. To prepare the FUdR plates, 33 µl from the stock concentration of 133 µM FUdR was mixed with 100 ml of NGM medium and poured in 60 mm plates. These plates were allowed to dry overnight in the hood and plated with bacteria.

## **2.1.3 Bacterial Strains**

### **2.1.3.1 *E. coli* OP50**

*E. coli* OP50 was the bacterial strain that was commonly used as the food for the worms. This strain is auxotroph for Uracil and has slow growth on Nematode Growth Media (NGM) plates. An overnight culture in LB was used to spread on the NGM plates and incubated at RT for overnight to form the bacterial lawn.

### **2.1.3.2 *E. coli* HT115**

This strain was primarily used for RNAi experiments. They have endogenous tetracycline resistance and defective dsRNA degradation machinery. It can express dsRNA corresponding to a gene of interest from the transformed plasmid with the gene fragment cloned in it.

## **2.2 Phenotypic Assays**

### **2.2.1 Lifespan Assay**

The worms were assayed for their lifespan under different conditions. 4-5 gravid worms of any strain were kept on a fresh plate containing normal food of OP50 or dsRNA expressing bacteria to lay eggs for exactly 3 hours. The adults were removed from the plate and the progenies were allowed to grow till the L4 stage. 30 worms were then shifted to the FUdR plates containing an ample amount of food. The worms were scored for their mortality every day and scored dead once they stopped responding to the touch with the platinum loop. For the RNAi experiments, the worms were shifted to fresh plates with the same composition after every four days until the total mortality.

The analysis of lifespan assay was performed either using OASIS or Prism5 software. Kaplan-Meier plot was made for every experiment and the median lifespan was calculated.

### **2.2.2 Temperature stress assay**

High temperature causes misfolding of proteins particularly in the cytoplasm. We tested for the resilience of the worms in the non-permissible temperature condition. Worms in the day 1 adult stage were put on the NGM plates devoid of any bacteria. 20 worms were put on one plate and incubated at 35°C (Oh et al., 2005). The worms were scored for their mortality every hour and considered death if there was no spontaneous movement or response when touched. The analysis of the experiment was done similar to that for the lifespan assay.

### **2.2.3 Oxidative stress assay**

Oxidative stress caused by the ROS causes misfolding of the proteins and affect mitochondria. The drug, TBHP is an external xenophytic agents and causes a high degree of protein misfolding in mitochondria. 20, day 1 adult worms were transferred to NGM plates containing 90 µl of TBHP (70% V/V Sigma Luperox TBH70X) per 100 ml of media. These plates were kept in 20°C and the worms were scored every hour for the mortality. The analysis was done similarly to the lifespan assay.

## **2.3 Molecular Biology**

### **2.3.1 DNA extraction and genotyping**

Worms were washed and harvested from one 60 mm NGM plate. The worms pellet was resuspended in the worm lysis buffer (50 mM KCl, 10 mM Tris (pH 8.3), 2.5 mM MgCl<sub>2</sub>, 0.45 % NP-40, 0.045 % Tween-20, 0.01 % (w/v) gelatin) and incubated at 55°C for 2 hours. The proteinase K was inactivated by incubating at 95°C for 20 min. The DNA was purified using phenol: chloroform: isoamyl alcohol (PCI) method. 500 µl of PCI was added to the solution and mixed well at RT. The tubes were spun at 20,000x g for 15 min and the top aqueous layer was collected in separate tubes. 0.8 volume of isopropanol and 0.1 volume of 2.5 M sodium acetate was added and incubated on ice for 1 h. After the incubation, the DNA was pelleted at 20,000x g for 20 min followed by

two washes with 75% (v/v) ethanol. The pellet was air-dried and resuspended in 30  $\mu$ l of NFW. The concentration of the genomic DNA was quantified using Nanodrop (ThermoFisher Scientific). The genotyping was performed with 30 ng of genomic DNA and the specific primers.

### **2.3.2 Worm Lysis and total protein extraction**

*C. elegans* have cuticle on their outer surface composed of collagen. Cuticle confers rigidity to the worms and prevents rupture from detergents. This makes the extraction of macromolecules like proteins and nucleic acids more tedious.

A synchronized or mixed population of worms were harvested from the NGM plates or liquid culture. The worms were given at least three washes with M9 buffer to remove bacteria. The worms were then suspended in the lysis buffer (25 mM Tris-HCl (pH 7.5), 100 mM NaCl, 0.5 % NP-40, 1 mM EDTA, 1 mM PMSF, 1x PIC) and flash-frozen in liquid nitrogen. The frozen worms were thawed on ice and sonicated with the probe sonicator for 1 min. The freeze-thaw-sonication cycles were repeated until the entire worm body was lysed. The membranous debris was pelleted down with high speed centrifugation and the supernatant was collected. The protein amount was quantified with the Pierce BCA protein assay kit (ThermoFisher, Cat No.23225).

### **2.3.3 Immunoprecipitation (IP) and Western blotting**

At least 1 mg of total protein was used for the IP. The protein lysate was incubated overnight at 4°C with 2  $\mu$ g of antibody against a particular protein of interest or IgG as isotype control. The lysate and antibody were incubated with magnetic Dyna beads for 4 hours at 4°C. The complex bead-antibody-protein complex was washed four times with the lysis buffer to remove the non-specific interactions with the protein. The beads were finally cracked by boiling in the 2x SDS dye to elute all the proteins.

The proteins were separated on acrylamide gel in the SDS running buffer and transferred on the PVDF membrane using the wet transfer protocol. The membrane was blocked with 5% skimmed milk in 1x TBST (20 mM Tris (pH 7.5), 150 mM NaCl,

0.1 % Tween 20). The primary antibody in standardized dilution in the blocking buffer was incubated on the blot overnight at 4°C. After the incubation, the blot was given four washes with 1x TBST and probed for 1 hour at RT with a secondary antibody raised against the animal in which the primary antibody was raised. Again four washes with 1x TBST were given to minimize the non-specific signal. The blot was developed using ImageQuant LAS 4000 (GE healthcare) with ECL western blotting substrate (Bio-Rad, Cat No.1705061).

### **2.3.3 Nuclear Cytoplasmic Fractionation**

The nuclear and cytosolic proteins were fractionated essentially according to Mata-Cabana et al., 2018. Approximately 50,000 worms were harvested and washed from either the NGM plates or liquid culture. The worms were resuspended in the hypotonic buffer (15 mM HEPES KOH pH 7.6, 10 mM KCl, 5 mM MgCl<sub>2</sub>, 0.1 mM EDTA, 350 mM Sucrose) and dounced vigorously till most worm bodies dissolved. The debris was spun down at 400x g for 5 min followed by 5000x g spin for 5 min to separate the nucleus. The cytosolic fraction in the supernatant was further centrifuged at 20,000x g for 15 min to remove membranous portion. Nuclear fraction was given multiple washes with the hypotonic buffer to remove any cytosolic contamination. The nucleus was then suspended in the high salt buffer (15 mM HEPES KOH pH 7.6, 400 mM KCl, 5 mM MgCl<sub>2</sub>, 0.1 mM EDTA, 0.1% Tween20, 10% Glycerol) and sonicated in bioruptor for 100 secs (20 sec ON/OFF, 5 cycles). The nuclear debris was pelleted at 20,000x g and supernatant was collected as the nuclear fraction. Proteins in both the fractions were quantified with the Pierce BCA protein assay kit (ThermoFisher, Cat No.23225).

### **2.3.4 Chromatin Immunoprecipitation (ChIP)**

ChIP was performed based on the protocol by Mukhopadhyay et al. 2008. Approximately, 100,000 worms were harvested, washed and crosslinked with 3 ml of Crosslinking buffer (1% (v/v) formaldehyde in 1x PBS) for 30 min at RT and gentle rocking. Formaldehyde was quenched using 2.5 ml of Glycine in a final concentration of 150 mM. The worms were washed four times with 1x PBS with 1x PIC (Roche). The

pellet was then resuspended using 2 ml of HLB (50mM HEPES-KOH, pH 7.5, 150 mM NaCl, 1 mM EDTA, 0.1% (wt/vol) sodium deoxycholate, 1% (vol/vol) Triton X-100, 0.1% (wt/vol) SDS, 1 mM PMSF and 1x PIC) and split in two aliquots for sonication. Sonication was performed at 4°C using Covaris m220. 35-40 sonication cycles (30 s ON/OFF) were performed to shear the chromatin to the size of 300-400 bp. The lysed cells and debris were centrifuged at 20,000x g for 15 min at 4°C to obtain the soluble cross-linked chromatin which was further diluted with HLB for further steps. 20-30 µg of chromatin was precleared with 20 µl of blocked protein G beads (protein G plus tRNA and BSA) for 2 h. Post incubation, the precleared samples were incubated overnight for the immunoprecipitation with 2 µg of specific antibody and isotype control at 4°C. After incubation, 20 µl of the blocked beads were added to the samples and kept on end-to-end rotation at 4°C for 3-4 h. The beads-antibody-TF-DNA complex were washed for 5 min at 4°C twice with low salt buffer, WB1 (50 mM HEPES-KOH, pH 7.5, 150 mM NaCl, 1 mM EDTA pH 8.0, 1% (w/v) sodium deoxycholate, 1% (v/v) Triton X-100, 0.1% (w/v) SDS and 1 mM PMSF), twice with high salt buffer, WB2 (50 mM HEPES-KOH, pH 7.5, 1 M NaCl, 1 mM EDTA, pH 8.0, 0.1% (w/v) sodium deoxycholate, 1% (v/v) Triton X-100, 0.1% (w/v) SDS), twice with WB3 (50 mM Tris-Cl, pH 8.0, 0.25 mM LiCl, 1 mM EDTA, 0.5% (v/v) NP-40 and 0.5% (w/v) sodium deoxycholate) and thrice with TE (10 mM Tris-Cl, pH 8.0, 1 mM EDTA). The chromatin-antibody complex was eluted in 300 µl of freshly made elution buffer (2% SDS and 0.1M NaHCO<sub>3</sub>). The reverse crosslinking was performed overnight at 65°C followed by 1 h of proteinase K (100 µg/ml) at 45°C. DNA was purified using the phenol: chloroform: isoamyl alcohol extraction and used for qPCR.

### **2.3.5 RNA Isolation from worms**

Worms were harvested and washed from 2-3 NGM plates using M9 buffer. The worm pellet was then resuspended in 1 ml trizol and immediately flash-frozen in liquid nitrogen. The samples were either stored in -80°C or proceeded further to thaw on ice. When the solution was partially melted, it was vortexed vigorously for 2 mins and flash-frozen again. This cycle was repeated at least 3-4 times until the worm bodies dissolved completely. 300 µl of chloroform was added and mixed gently for the

organic-aqueous phase separation. The tubes were centrifuged at 20,000x g for 15 min and the aqueous layer was collected in separate tubes. The chloroform step was repeated to remove any trizol contamination. 0.8 volume of Isopropanol was added to the solution and incubated on ice for 1 hour. Further RNA was precipitated by centrifugation at 20,000x g for 20 min, followed by two washes with 75 % ethanol. The RNA pellets were air-dried till droplets of ethanol evaporated and the pellets were resuspended in 30 µl of NFW. The concentration of RNA was quantified using NanoDrop (ThermoFisher Scientific).

### **2.3.6 DNase treatment of isolated RNA**

The DNase treatment is essential to remove any residual DNA present in the isolated RNA sample. We used the Promega RQ1 DNase kit (Catalog No. M6101) for this. For every 20 µl reaction, the reaction mix contained 2 µg of RNA, 1 µl of RQ1 DNase buffer and 1 µl of RQ1 DNase and incubated for 45 min at 37°C. The reaction was stopped by adding 1 µl of stop solution and incubated at 65°C for 20 min. The concentration of RNA was quantified using NanoDrop.

### **2.3.7 cDNA synthesis**

For the cDNA synthesis, we used the Promega cDNA synthesis kit (Cat No. A3500). For 20 µl of reaction, 1 µg of DNase treated RNA, 2 µl of RT buffer, 0.3 µl of random primers, 0.3 µl of dNTP mix, 1 µl of Reverse transcriptase and NFW to make up the volume was mixed in a PCR tube. The protocol used in the thermocycler was: 25°C for 10 min, 37°C for 120 min, 85°C for 5 min and 4°C for storage. The cDNA synthesis was confirmed with a PCR reaction using the primers for a control gene, *yr45f10d*.

### **2.3.8 Quantitative real-time PCR**

For the quantification of transcripts, we used quantitative real-time PCR (qRT-PCR). The reaction mix for every 10 µl reaction contained 5 µl of SYBR mix (Sigma, Cat No.



KK4601), 1 µl of cDNA template (1:4 diluted in NFW), 0.2 µl of 10 uM primer mix and 3.8 µl of NFW. PCR was performed using Bio-Rad CFX96 thermal cycler with the protocol as follows:

Denaturation: 95C for 5min

Denaturation: 95C for 15sec  
Annealing: 60C for 30sec  
Extension: 72C for 30sec

} 40 cycles

Storage: 4C

The differential gene expression was calculated using the  $\Delta\Delta Ct$  method. The Ct value obtained for every gene target for a template sample was normalized with the Ct obtained for the control gene, *yr45f10d* for the same template to obtain  $\Delta Ct$ .  $\Delta\Delta Ct$  was obtained for each target and sample by subtracting with corresponding  $\Delta Ct$  for the target with that of control sample. The fold change was calculated using the formulae,  $2^{(-\Delta\Delta Ct)}$ .

For quantification after ChIP, the DNA from the ChIP with antibodies against TFs was directly used as template for the q-PCR while the input DNA template was diluted 10 times with NFW. The quantification for the enrichment of TFs at the particular genomic loci was done using the following formulae:

$$\% \text{ (ChIP/ Total input)} = 2^{[ \text{Ct (x\% input)} - \log(x\%)/ \log 2 - \text{Ct(ChIP)} ]} \times 100\%$$

Here, Ct (ChIP) and Ct (x% input) are threshold values obtained from exponential phase of qPCR. The compensatory factor ( $\log x\% / \log 2$ ) is used to take into account the dilution 1: x of the input. The recovery is the % (ChIP/ Total input).

Relative occupancy can be calculated as a ratio of specific signal over background:

$$\text{Occupancy} = \% \text{ input (specific loci)} / \% \text{ input (background loci)}$$

### 2.3.9 Antibodies

The antibody against DAF-16 was a kind gift from Dr Arnab Mukhopadhyay (NII, New Delhi). The monoclonal antibody against DVE-1 was home-raised in mouse. Normal

rabbit IgG (12-370) and Normal mouse IgG (12-371) for ChIP were procured from Millipore (Massachusetts, USA). Anti-GAPDH antibody (0411) was purchased from Santa Cruz Biotechnology (Texas, USA).

### 2.3.10 Primers

Primer Name	Sequence 5' to 3'	Purpose
<i>C. elegans</i> Daf-12-F	CAACAAACGTGCGGCATACA	qPCR
<i>C. elegans</i> Daf-12-R	ATTGCCTGGAATGGCTGACA	qPCR
<i>C. elegans</i> Daf-16-F	AGGAGAGAGCATTGATGGGC	qPCR
<i>C. elegans</i> Daf-16-R	GATTGAGTTCGGGGACGGAA	qPCR
<i>C. elegans</i> Daf-2-F	CTTTTGTACAGCCGTGTGCC	qPCR
<i>C. elegans</i> Daf-2-R	ACCACTGTGCAGTTGACCAT	qPCR
<i>C. elegans</i> -Y45F10D.4-F	CATTCGGATGTGGAAGTGCAA	qPCR CONTROL
<i>C. elegans</i> -Y45F10D.4-R	TCTTGGGCGAGCATTGAACA	qPCR CONTROL
<i>C. elegans</i> sod-3-F	GGAGAACTTCACGAGGCTGT	qPCR
<i>C. elegans</i> sod-3-R	AGTCGCGCTTAATAGTGCCA	qPCR
<i>C. elegans</i> DAF-2 GENOTYPING FP	CGGGATGAGACTGTCAAGATTGGAGATTTCCGG	Genotyping
<i>C. elegans</i> DAF-2 GENOTYPING RP	CAACACCTCATCATTACTCAAACCAATCCATG	Genotyping
<i>C. elegans</i> DAF-16 Forward Primer	CAATGAGCAATGTGGACAGC	Genotyping
<i>C. elegans</i> DAF-16 Reverse Primer	CCGTCTGGTCTGTCTTTT	Genotyping
<i>C. elegans</i> HSP-4 Forward Primer	GGCAAACGCGTACTGTGATG	q-PCR
<i>C. elegans</i> HSP-4 Reverse Primer	CTGTTTCTTGATCGTTGGCG	q-PCR
<i>C. elegans</i> HSP-60 Forward Primer	GAAAGGGACTTCAGACCGCC	q-PCR
<i>C. elegans</i> HSP-60 Reverse Primer	GATCACGTTTCTTCTTTTGGGC	q-PCR
<i>C. elegans</i> HSP-6 Forward Primer	CAACGATTCTCAGCGTCAAGC	q-PCR
<i>C. elegans</i> HSP-6 Reverse Primer	AGCGATGATCTTATCTCCAGCG	q-PCR
<i>C. elegans</i> HSP-16.11 FP	GTCTCGCAGTTCAAGCCAGA	q-PCR
<i>C. elegans</i> HSP-16.11 RP	ACCAACATCAACATCTTCGGGT	q-PCR
<i>C. elegans</i> DVE-1 cDNA Geno FP	TGGTTCACACAAAACGCTCG	Genotyping
Dve-1 RNAi FP	GACTGATATCAAGGGAAACATTGAAAAACCATT	RNAi
Dve-1 RNAi RP	GAGCGATATCCACTCTTACGAAATCCACGTC	RNAi
CCO-1 RNAi FP	GACTGATATCtggtcaactgctaagacgg	RNAi
CCO-1 RNAi RP	GACTGATATCtagatggattctgggtcggc	RNAi
Hsp-60 promoter FP	TCAGTCATTACCTGCTTCCAGACG	ChIP
Hsp-60 promoter RP	CCTTTCTGGCGAGGCGAAGCATCT	ChIP
Hsp-6 promoter FP	CAAACCTCTGTGTCAGTATCATGGAAGG	ChIP
Hsp-6 promoter RP	GCTGGCTTTGACAATCTTGATGGAACG	ChIP
Dve-1 FP(Exon1-2 Junction)	CATGCTCAAACGAAGGACACA	qPCR
Dve-1 RP (Exon1-2 Junction)	TATGAGGCCTCGAGCACTTG	qPCR
Daf-16 FP (Exon1-2 Junction)	GAACTGTCGTGAGCTCGATTC	qPCR
Daf-16 RP (Exon1-2 Junction)	CCGAACGCTCTTGTGATGG	qPCR

# Chapter 3

## DAF-16 interacts with DVE-1

### 3.1 Introduction

The lifespan of an organism depends on its ability to tackle the environmental and metabolic insults that it faces during its lifetime. The usual mechanism through which it is achieved is by modulating the transcriptional paradigm in the cells, tuning the gene expression pattern for the effective response (Kenyon, 2010). Insulin signaling has been studied to play an important role in the development and longevity of *C. elegans*. Primarily acting as the nutrition-sensing pathway, the absence of food turns off Insulin signaling leading to the nuclear localization of the TF, DAF-16 which then brings about the requisite transcriptional changes and dauer formation (Gottlieb and Ruvkun, 1994a; Kondo et al., 2005). Besides this, other stress response pathways like that against temperature, ROS or pathogen have also been found to be partially dependent on DAF-16 (Oh et al., 2005; Volovik et al., 2014). But the question which arises is whether DAF-16 mediated response enough to counter such wide range of stress condition on itself? Recent studies have shown other TFs that act together with DAF-16 under different stress conditions modulate these transcriptional changes (Lin et al., 2018; Tepper et al., 2013). Here in this study, we show that the DVE-1, the SATB1 homolog in *C. elegans* interact with DAF-16 and can potentially change the expression level of various genes.

### 3.2 Results

#### 3.2.1 DVE-1 and DAF-16 have common genomic targets

The modERN (model organism Encyclopedia of Regulatory network) consortium combined the data from modENCODE (Model Organism Encyclopedia of DNA Elements) with the new ChIP-sequencing data for other transcription factors (Kudron et al., 2018). There is genome binding information of about 262 TFs of the fly genome and 217 TFs of the worm genome. We obtained the raw ChIP-sequencing data from modERN consortium for DVE-1 and DAF-16 and analyzed them. We found over 60 percent of all the genes that these two transcription factors bind to be common between them. Also, about 24 percent of genes were exclusive bind targets of DAF-16 and about 13% were that of DVE-1 (Fig.3.1A). We also analyzed the average

binding profile of the TFs using Deeptools to plot their general occupancy across any target gene.

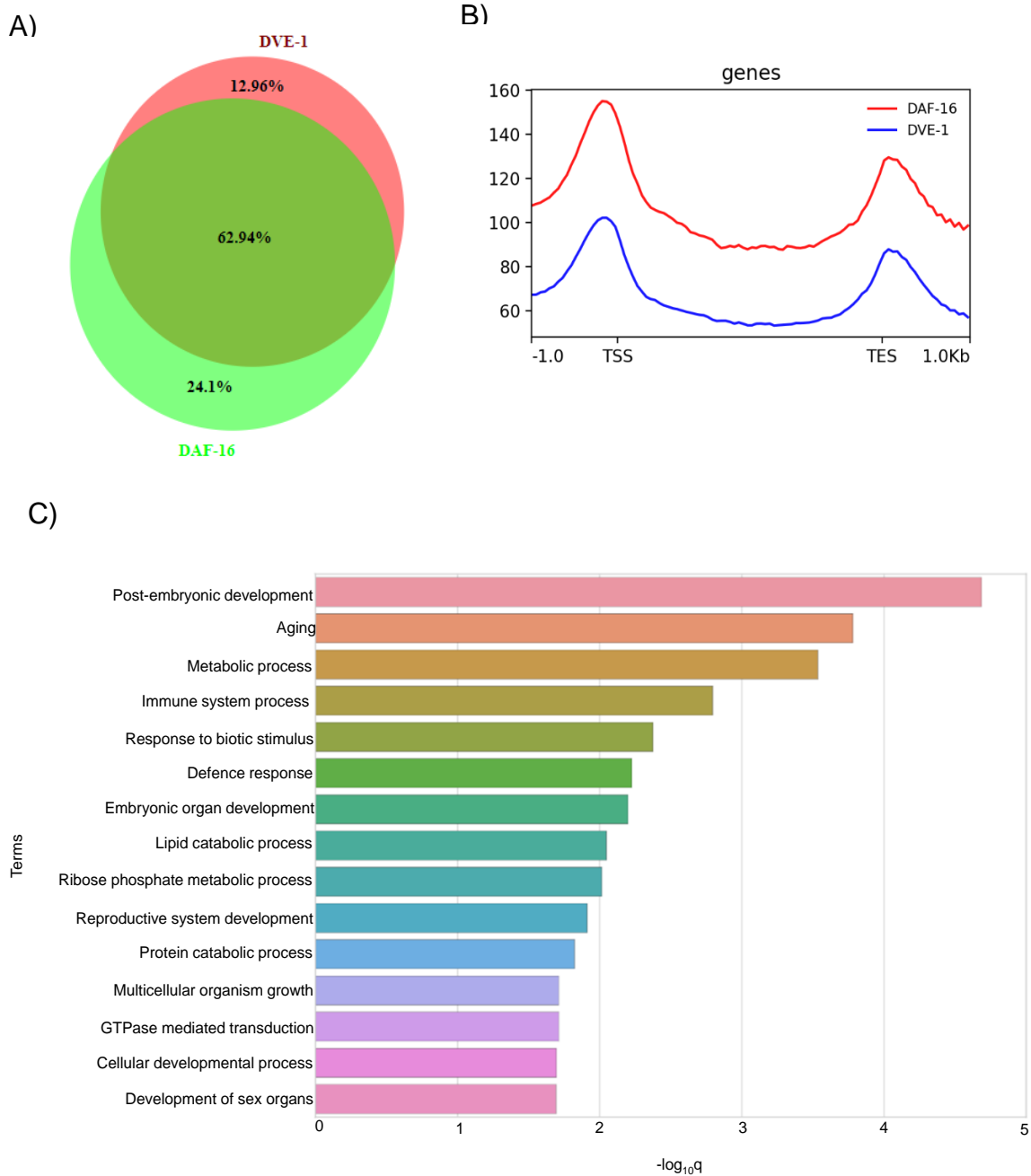


**Figure 3. 1. DVE-1 and DAF-16 share common targets on the genomic loci.**

(A) ChIP-sequencing analysis showed large number of common gene targets of DVE-1 and DAF-16. (B) DVE-1 and DAF-16 have similar global binding pattern on the genome. Both TFs show binding at the promoters and 200bp downstream of TES. (C) The GO-term analysis of the common genes indicated several biological pathways including ageing which could be affected with the binding of DVE-1 and DAF-16 together on the genome.

Interestingly, the occupancy peaks of the TFs exactly overlapped with one another. The peaks were primarily on the promoter of target genes and 200bp downstream of the transcription end site (Fig. 3.1B). The Pearson correlation of the binding sites was 0.75, indicative of their co-occupancy on the genomic loci. Further, we performed the gene-enrichment analysis of the target genes. These genes were found to be involved in several biological pathways like metabolic process, ageing, binding profile of the TFs using DeepTools to plot their general occupancy across any defence, etc. (Fig. 3.1C).

### 3.2.2 Validation of monoclonal antibody raised against DVE-1

For in vivo investigation of this interaction, we used mouse monoclonal antibody against DVE-1 which was previously raised in the lab by Dr. Manjunath. We validated the antibody for its avidity and specificity by western blotting. *dve-1* was knockdown in the wildtype worms by the genes specific RNAi and total protein was isolated at the Day1 adult stage. We observed a complete loss of the 53kDa band which is the expected size of DVE-1(Fig. 3.2(1)). The RNAi didn't affect the expression level of the control protein, GAPDH (Fig. 3.2 (2)). Being a serum antibody, we did observe some nonspecific bands at sizes higher than that of DVE-1. We previously suspected them to be post-translationally modified form of DVE-1 (Gao et al., 2019) but they were also present after knockdown of *dve-1*. Thus we confirmed that the serum antibody does recognize the band for DVE-1 at 53 kDa size.

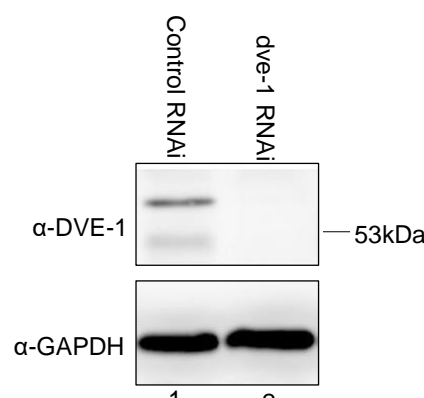


**Figure 3. 2. Confirmation of the specificity of the home-raised monoclonal antibody.**

The 53 kDa band for DVE-1 was completely lost upon feeding the worms with HT115 bacteria induced for the generation of dsRNA against *dve-1* mRNA (2).

### **3.2.3 Localization of DVE-1 and DAF-16 in the subcellular compartment**

So as to study the interaction and complex formation of DVE-1 and DAF-16, we standardized the conditions in which both the TFs localized in nucleus. The absence of Insulin signaling or stress conditions like high temperature or ROS in the cells lead to the nuclear localization of DAF-16. (Hsu et al., 2003; Wu et al., 2018). DVE-1 is reported to translocate to nucleus under mitochondrial stress (Haynes et al., 2007). As common location of the partners will facilitate the active complex formation, we wanted to understand the subcellular localization of Dve1 and DAF16 under heat stress and dietary restriction.

We used the TJ356 strain which had DAF-16-tagged with GFP and grew these strains in liquid culture media with caloric restriction. One set of cultures was given a heat-shock of 30 minutes at 35°C while the other set was kept as a control for heat stress. Using a standardized protocol for protein fractionation, we could isolate the nuclear and cytosolic fractions of proteins, separately. We performed western blotting and probed with anti-DVE-1 or anti-GFP antibody along with the antibodies against the known markers of the two subcellular fractions. We found that under both temperature stress and dietary restriction, the localization of DVE-1 and DAF-16 was nuclear (Fig. 3.3).

DAF-16 being attached with 14-3-3 chaperone proteins is inactive in the cytoplasm and so is DVE-1 which is post-translationally SUMOylated (Gao et al., 2019). Thus if there were an interaction between them, we expected it to be in the nucleus and not in the cytoplasm. This culture condition rendered the nuclear localization of both TFs and ideal for their co-immunoprecipitation to confirm the interaction.

### **3.2.4 DAF-16 co-immunoprecipitates with DVE-1 and vice-versa**

With the culture condition used for the localization experiment, we again used the TJ356 stain and isolated the total protein from the mixed-population of worms. We performed immunoprecipitation using anti-DVE-1 antibody and probed with the anti-GFP antibody. We observed the band for the GFP-tagged DAF-16 at the 90kDa size, indicative of its co-immunoprecipitation with DVE-1 (Fig. 3.4A).

To further validate this interaction, we performed reverse immunoprecipitation from the total protein extract using anti-GFP antibody and probed with the anti-DVE-1 antibody. We did observe the band for DVE-1 at its correct molecular size, confirming its direct or indirect interaction with DAF-16 (Fig. 3.4B).

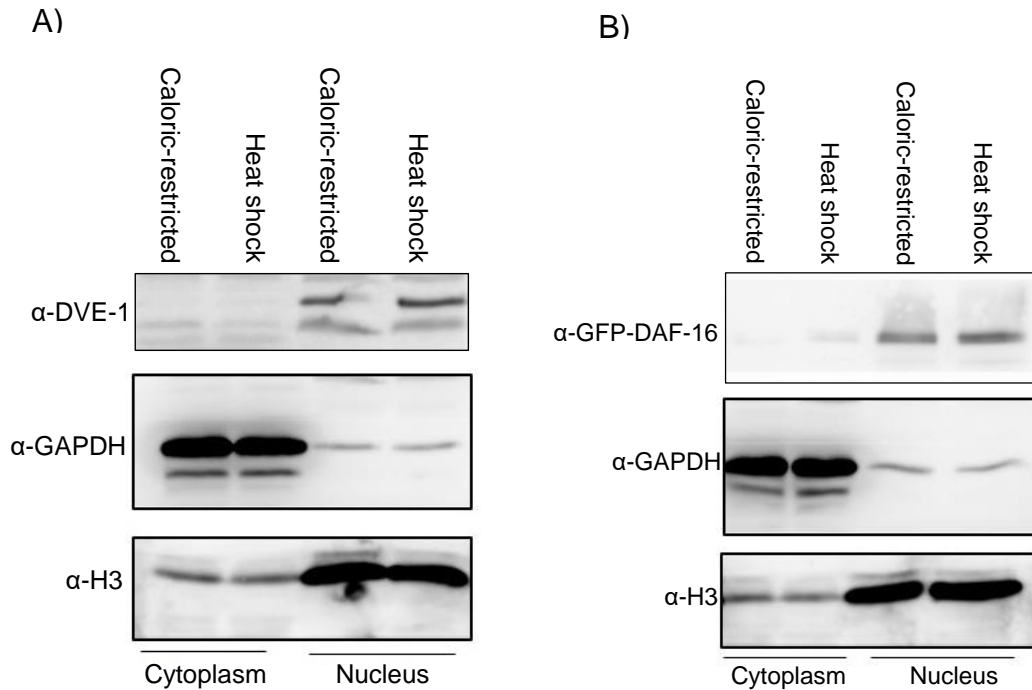


**Figure 3. 4. Effect of temperature and CR on the localization of DVE-1 and DAF-16.**

(A) The band for DVE-1 remains predominantly in nuclear fraction in both temperature stress and caloric-restriction. (B) DAF-16 like DVE-1 was also found in the nuclear fraction in both the treatment condition.

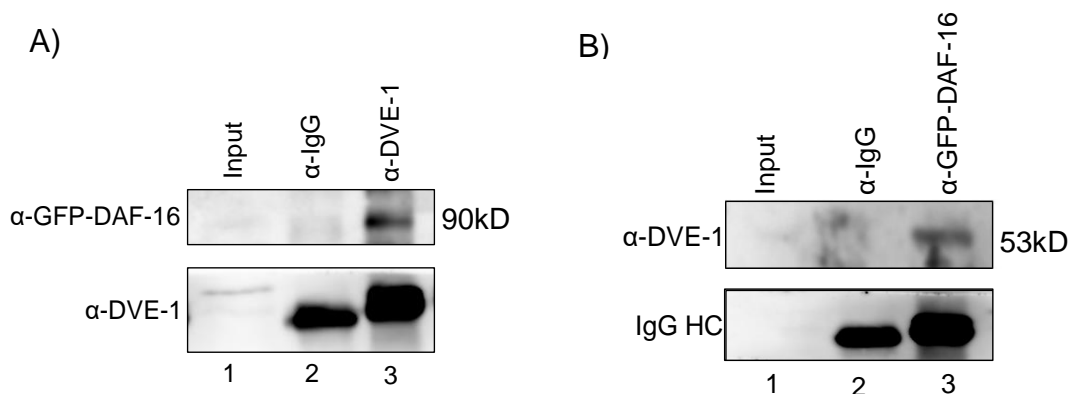


**Figure 3. 3. DVE-1 and DAF-16 interact with each other.**

(A) Probing with anti-GFP antibody to the IP with anti-DVE-1 antibody showed the band for GFP-DAF-16 at 90kDa. (B) Reverse IP with anti-GFP antibody was probed with anti-DVE-1 antibody confirmed the interaction of the two TFs.



### 3.2.5 Confirmation of the interaction of DVE-1 and DAF-16 on chromatin

Next, we asked whether these two TFs have interaction on the chromatin and if they bound on the target genes as a complex? To investigate this, we used Chromatin Immunoprecipitation (ChIP) followed by quantitative PCR for some genomic loci which we knew to be common targets of the TFs from the previously analyzed ChIP-sequencing data.

#### 3.2.5.1 Standardization of shearing of Chromatin from worms

Shearing of the chromatin is one of the important steps in ChIP and we standardized it for an efficient IP. We again used the TJ356 strain grown in the liquid culture as the previous experiments. The shearing was performed for different numbers of cycles of pulses and later checked on the agarose gel after decrosslinking. We found 40 cycles of pulse was optimum for shearing the chromatin and was used in the further ChIP experiments (Fig. 3.5).

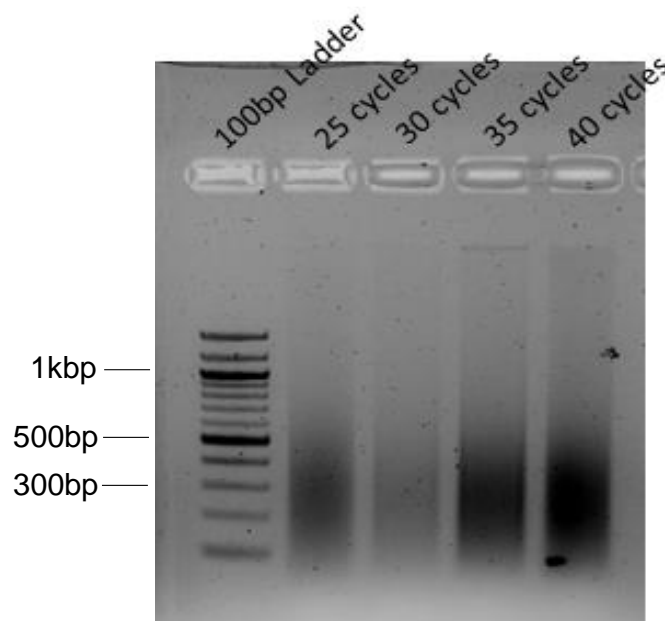


**Figure 3. 5. Optimization of sonication for the shearing of the chromatin from worms.**

40 cycles of sonication was optimum for shearing the worm chromatin to the size of 200-300bp.

### 3.2.5.2 DAF-16 and DVE-1 binds to the promoters of *hsp-6* and *hsp-60*

We performed ChIP using the antibodies against DVE-1, DAF-16, and normal mouse IgG as the antibody isotype control. We checked for the enrichment of DVE-1 and DAF-16 on the promoters of the known targets of DVE-1, *hsp-6*, and *hsp-60*. The enrichment of DVE-1 on *hsp-6* promoter was less compared to that of *hsp-60*. Interestingly, DAF-16 showed higher enrichment on both the promoters (Fig. 3.6).

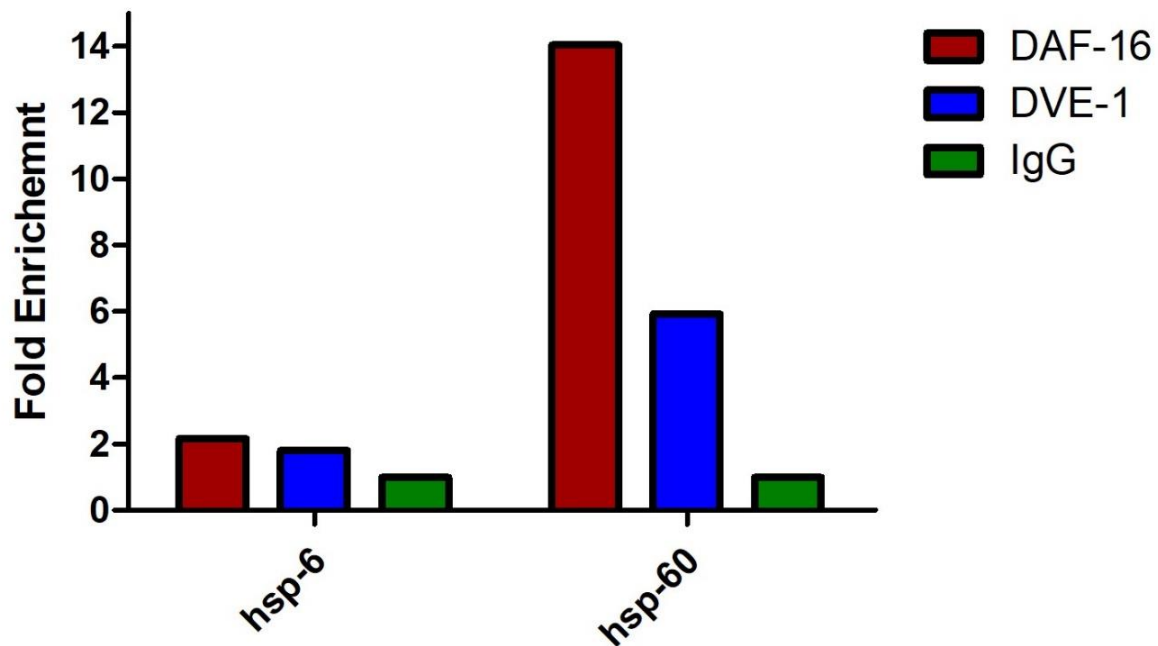


**Figure 3. 6. Enrichment of DVE-1 and DAF-16 on the promoters of *hsp-6* and *hsp-60*.**

On the promoter of *hsp-6*, DVE-1 and DAF-16 had almost two-fold enrichment compared to the control. While on the promoter of *hsp-60*, DAF-16 and DVE-1 had much stronger occupancy of several folds.

### 3.2.5.3 DAF-16 co-immunoprecipitates with DVE-1 in ChIP

Finally, to confirm the interaction of DVE-1 with DAF-16 on the chromatin, we performed the western blotting after the immunoprecipitation of sheared chromatin with the antibody against DVE-1 and probed with  $\alpha$ -GFP. We obtained the band for GFP-tagged DAF-16 at 90kDa size, confirming the complex formation of DVE-1 and DAF-16 that binds to the common genomic targets (Fig. 3. 7).

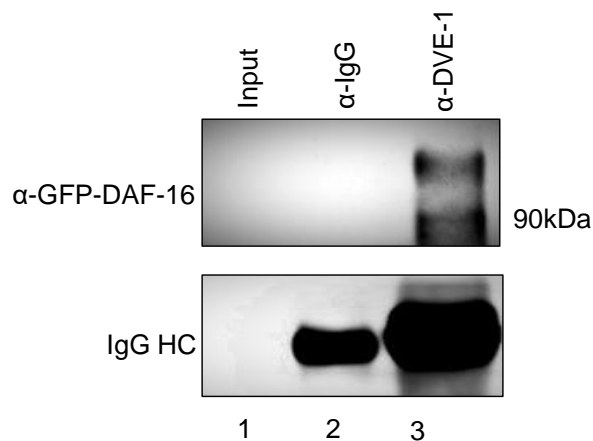


**Figure 3. 7. DAF-16 co-immunoprecipitated with DVE-1 after Chromatin immunoprecipitation.**

α-GFP antibody was probed on the blot after the immunoprecipitation of chromatin with α-DVE-1 antibody. The band at 90 kDa confirmed the co-immunoprecipitation of DAF-16.

### 3.3 Discussion and future directions

We began with the bioinformatics analysis of the ChIP-sequencing data of DVE-1 and DAF-16 to find that the two TFs exhibit a significant number of common targets. Their global binding profile also had an uncanny resemblance to each other. The occupancy peaks were centered at the promoters of the target genes or downstream of the transcription end site. DAF-16 is known to bind to the promoters of the target genes to change their expression level (Lee et al., 2003). Similarly, DVE-1 binds to the promoters of mitochondrial chaperone genes to upregulate their expression level (Haynes et al., 2007). DVE-1 is the *C. elegans* homolog of the mammalian SATB family of proteins, the master chromatin regulators which have known roles in development (Savarese et al., 2009), immune cell differentiation (Gottimukkala et al., 2012; Khare et al., 2019), X-chromosome inactivation (Agrelo et al., 2014; Nechanitzky et al., 2012) and oncogenesis (Mir et al., 2012; Wang et al., 2012). Like SATB1/SATB2, DVE-1 might have a different effect on the gene expression based on the binding site on any gene. It could also act as a cis-regulating element by binding at the intragenic regions as found in the ChIP-sequencing.

In a previous in-vitro protein interaction studies in the Galande lab by Manjunath et al., it was shown that huSATB1/SATB2 had direct interaction with the FOXO family of

proteins. Also, in the luciferase assay, SATB1 was found to be a negative regulator of the Insulin Responsive Elements (IREs). With the bioinformatics data and the molecular biology studies in the mammalian homologs, we hypothesized that DVE-1 and DAF16 interacted with each other directly or indirectly which affected the gene expression pattern crucial for the longevity of the organism.

We started with co-immunoprecipitation studies and used the home-raised antibody against DVE-1 and GFP-tagged DAF-16 strain. We showed that DAF-16 co-immunoprecipitated with DVE-1 and vice-versa. This was the first confirmation of our hypothesis and in line with the previous interaction studies of the mammalian counterparts of the two TFs. We also wished to understand if this complex bound to the chromatin and modulated the expression of the target genes. Therefore we performed chromatin Immunoprecipitation using antibodies against both TFs, followed by the quantitative PCR with the primers that spanned the genomic region at the promoters of *hsp-6* and *hsp-60*. We found that DAF-16 immunoprecipitated with DVE-1 along with the target chromatin. Further, the TFs exhibited strong occupancy on the promoters of the mitochondrial chaperone genes.

This binding can have a context-dependent synergistic or antagonistic effect on the gene expression of the target genes. For instance, under the unstressed condition, the expression level of *hsp-60* is slightly downregulated in *daf-2* (e1370) mutants (Wu et al., 2018). On the other hand, *dve-1* RNAi reduces the lifespan of not only the WT worms but also *daf-2* mutants (Durieux et al., 2011). Further investigations have to be made to fully understand the biological implications of this interaction. We plan to use the mutants of DAF-16 and DVE-1 or RNAi of these genes to characterize the conditions in which the interaction takes place and changes in the global transcription that would take place if this was inhibited.

## Chapter 4

A mutation in *dve-1* confers  
longevity to *C. elegans*

## 4.1 Introduction

In our previous study, we investigated the interaction between DVE-1 and DAF-16. But less is known about the other roles of DVE-1 in development and ageing of *C. elegans*. The reason for this is primarily due to the embryonic lethality upon knockout of *dve-1* (Haynes et al., 2007) such that any phenotypic characterization and ageing studies have been limited to RNAi. The knockdown of the gene reduces the lifespan of the wildtype worms and also the long-lived mutants (Durieux et al., 2011), indicative of its role in the development and maintenance of normal physiology of worms. To study this, we used a viable mutant strain of *dve-1* which had a deletion (allele name: *tm4803* and the mutant worms will be represented as *dve-1<sup>tm4803</sup>*) in the gene body and investigated its effect on the stress response and longevity. We found that this mutation not just conferred the longer lifespan to the worms but also increased their tolerance towards temperature and oxidative stress.

## 4.2 Results

### 4.2.1 The *tm4803* allele of *dve-1* conferred longevity and higher stress tolerance to *C. elegans*

*dve-1<sup>tm4803</sup>* harbors a deletion of 509 base pairs spanning the sixth exon and sixth intron at the ZK1193.5 loci. We confirmed the genotype of the mutant worm using PCR with the primer specific to this deletion. We observed a single band of about 400bp for the *dve-1<sup>tm4803</sup>* compared to the 1000bp band for N2, confirming the homozygous deletion in *dve-1* (Fig. 4.1A). We also confirmed the translation of the mutant ORF by western blotting and probed with the antibody against DVE-1. We observed the band for the truncated protein (DVE-1<sup>*tm4803*</sup>) at the expected size of 39 kDa (Fig. 4.1B).

We performed the domain analysis of the mutant DVE-1. DVE-1<sup>WT</sup> had a conserved N-terminal PDZ-domain that might interact with other transcription factors including UBL-5. There were also two other homeobox domains which would facilitate the binding on the chromatin. But unlike its homolog in the higher model system, SATB1/SATB2, it is devoid of CUT domains. The domain analysis for DVE-1<sup>*tm4803*</sup>

predicted an intact PDZ domain and only one of the homeobox domains. But due to the deletion, the protein lost the C-terminal Homeobox domain (Fig. 4.2B).

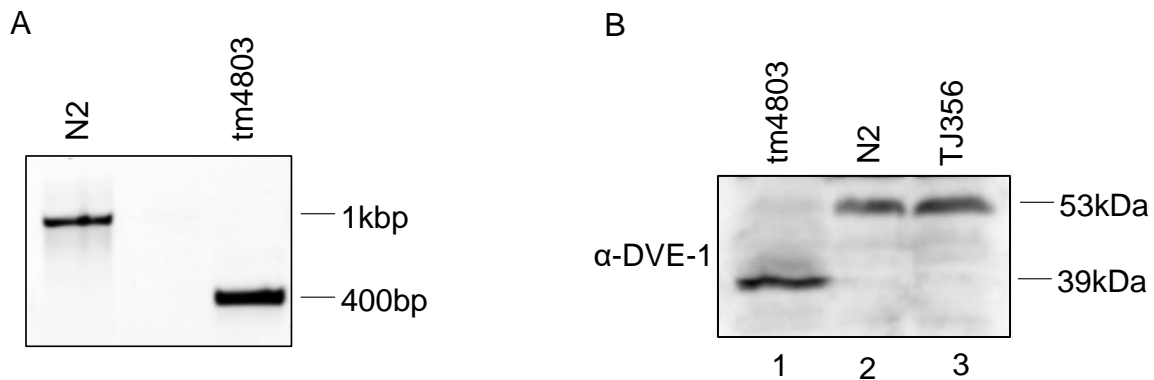


**Figure 4. 1. *dve-1<sup>tm4803</sup>* has homozygous deletion in *dve-1*.**

(A) The agarose gel image shows the 400bp PCR product for *dve-1<sup>tm4803</sup>* compared to 1000bp product for N2 confirming the deletion in *dve-1* gene. (B) Total protein was extracted from the worms and analysed using western blotting using the anti-DVE-1 antibody (1) *dve-1<sup>tm4803</sup>* translated into the truncated DVE-1<sup>*tm4803*</sup> of the 39kDa size. (2) N2 worms and (3) TJ356 (*daf-16::gfp*) translated full-length DVE-1 of 53 kDa.

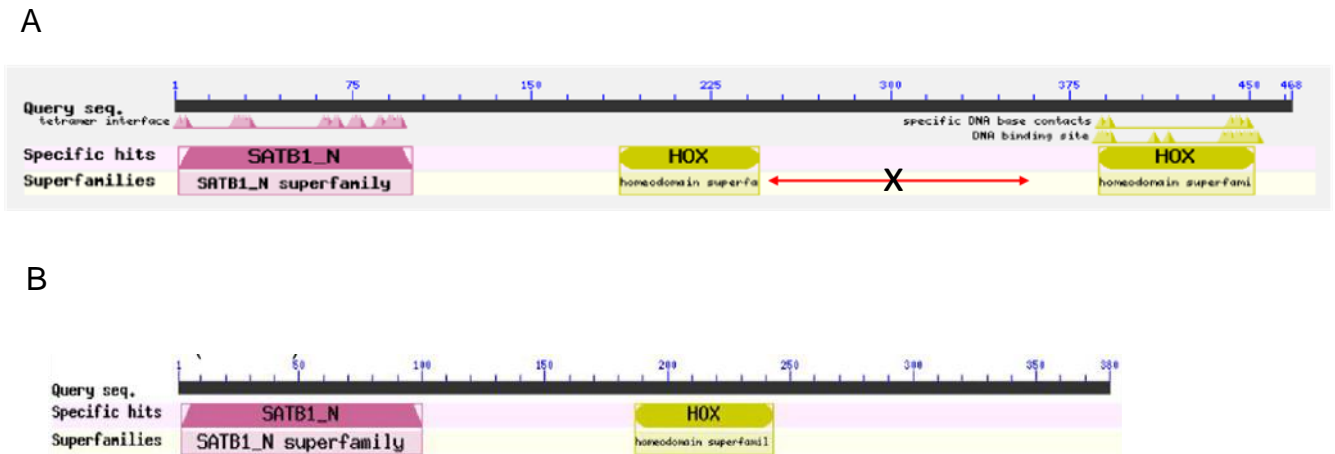


**Figure 4. 2. Domain architecture of DVE-1<sup>WT</sup> vs DVE-1<sup>tm4803</sup>.**

(A) DVE-1<sup>WT</sup> has N-terminal PDZ-domain and two HOX-domains. (B) 509bp deletion led to frame-shift in mRNA sequence with the complete loss of C-terminal Hox-domain.

#### 4.2.2 Phenotypic characterization of *dve-1<sup>tm4803</sup>* mutant worms

Next, we wanted to understand if this mutation in *dve-1* had any effect on the lifespan of worms. We performed the lifespan assay of *dve-1<sup>tm4803</sup>* worms and compared it to that of N2. Surprisingly, we observed a significantly increased median lifespan of *dve-1<sup>tm4803</sup>* of 21 days compared to 14 days of N2 (Fig. 4.3). Longevity and stress response are often positively correlated and long-lived mutant worms like *daf-2* (e1370) mutant show very high-stress resilience (Oh et al., 2005). We assayed the worms for their resilience to oxidative and thermal stress. The worms were grown on the NGM plate containing 12.5 mM of TBHP (tert-Butyl Hydroperoxide). TBHP generates ROS that permeates in the cells to cause misfolding of the proteins mostly in mitochondria. *dve-1<sup>tm4803</sup>* like other long-lived worms showed a robust response to the oxidative stress compared to N2 and short-lived *daf-16* null mutant worms, mgDf50 (Fig. 4.4A). Similarly, when the worms were incubated at 35°C, *dve-1<sup>tm4803</sup>* were much more resilient to the thermal stress than the other two strains (Fig. 4.4B). Thus, this deletion mutation in *dve-1* led to a higher lifespan and stress tolerance to the worms.

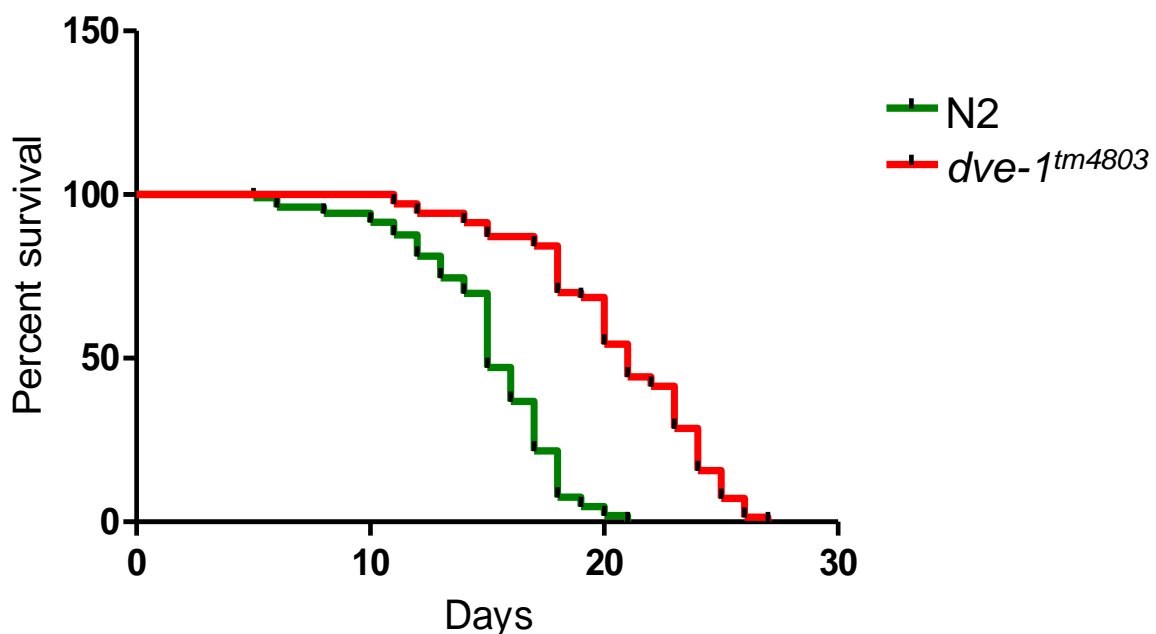


**Figure 4. 3. Lifespan assay of *dve-1<sup>tm4803</sup>* and N2.**

Kaplan-Meier plot showing the lifespan of two strains of worms: *dve-1<sup>tm4803</sup>* had the median lifespan of 21 days compared to 14 days of N2. P-value <0.0001 (Mantel-cox test).



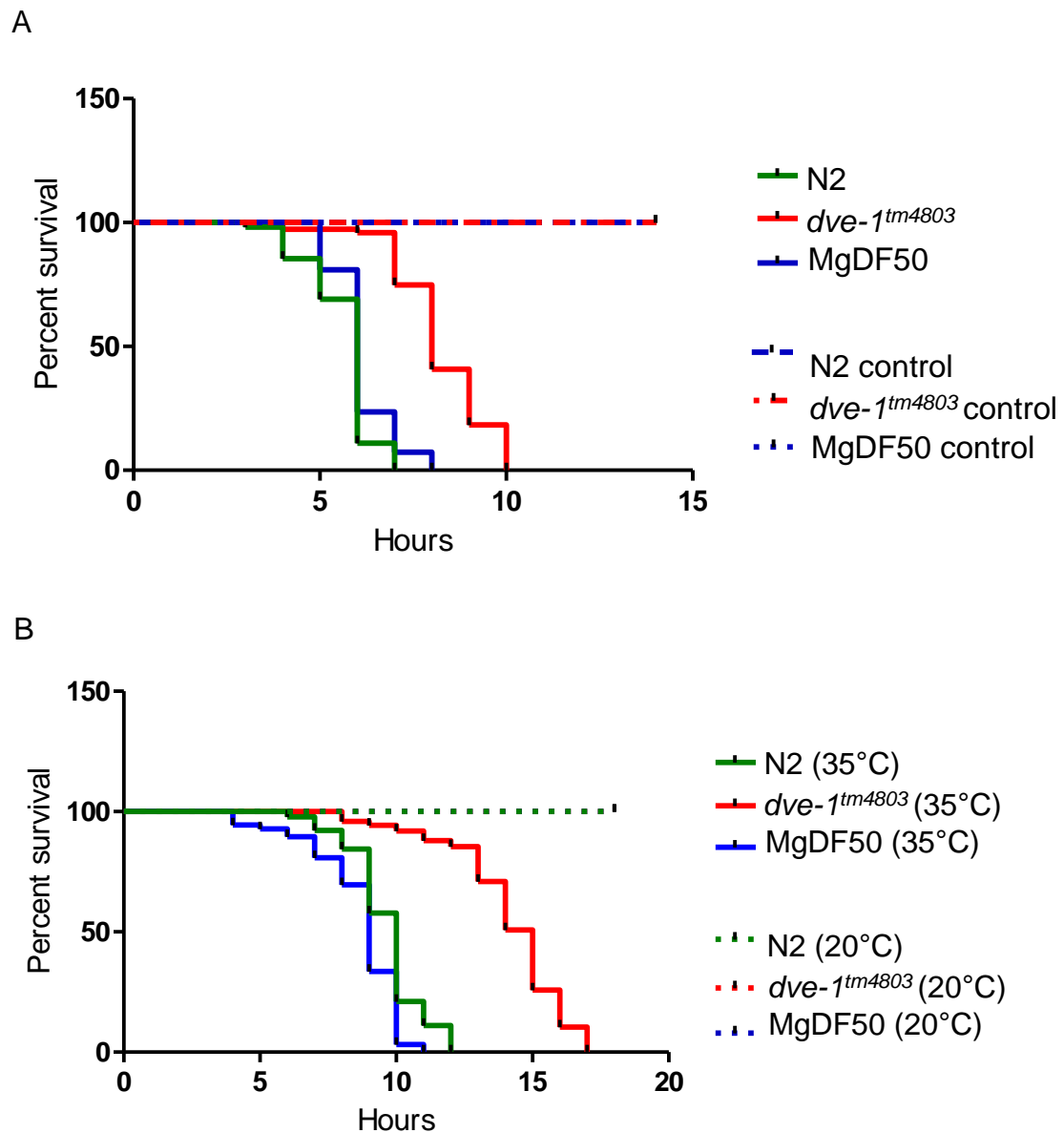


**Figure 4. 4. Oxidative and thermal stress assay of worms.**

(A) The worms were grown on NGM plates containing 12.5 mM of TBHP to expose the worms to oxidative stress. The survivorship curve shows the resilience of different strains of worms grown on TBHP plate vs the normal growth medium. No worm of any of the three strains died on control NGM plate till 15 hours of observation time. While on the TBHP plates, the median lifespan was 8 hrs for *dve-1<sup>tm4803</sup>*, 6 hrs for both N2 and mgDf50. P-values < 0.0001 (Mantel-cox test) (B) Thermal stress was given by incubating the worms at 35°C till all the animals died. The median survival of the worms was 15 hrs for *dve-1<sup>tm4803</sup>*, 10 hrs for N2 and 9 hrs for mgDf50. There was no mortality of the worms in the control condition of 20°C. P-values < 0.0001 (Mantel-cox test)

### 4.2.3 The *dve-1<sup>tm4803</sup>* allele doesn't form dauer at the non-permissive temperature

Dauers are developmentally arrested state of worms in which they cease to develop into reproductive adults. They are long-lived and highly resilient to stress conditions. There have been different pathways studied for the development of dauers (Gerisch et al., 2001; Gottlieb and Ruvkun, 1994b). The deficiency of Insulin/IGF-1 signaling has been one of the well-characterized pathways that leads to dauer formation. *daf-2* mutants at 25°C constitutively form dauers in a DAF-16 dependent fashion (Gems et al., 1998). As shown in our previous study that DVE-1 and DAF-16 interact with each other, we wanted to investigate if *dve-1<sup>tm4803</sup>* like *daf-2* mutant also formed dauers at 25°C. We performed dauer formation assay in which worms in the L1 stage were incubated at 25°C and the percent dauer formation was quantified. Only a small proportion of *dve-1<sup>tm4803</sup>* worms formed dauer even at 25°C unlike *daf-2* (*e1370*) that underwent 100% dauer formation at 25°C.

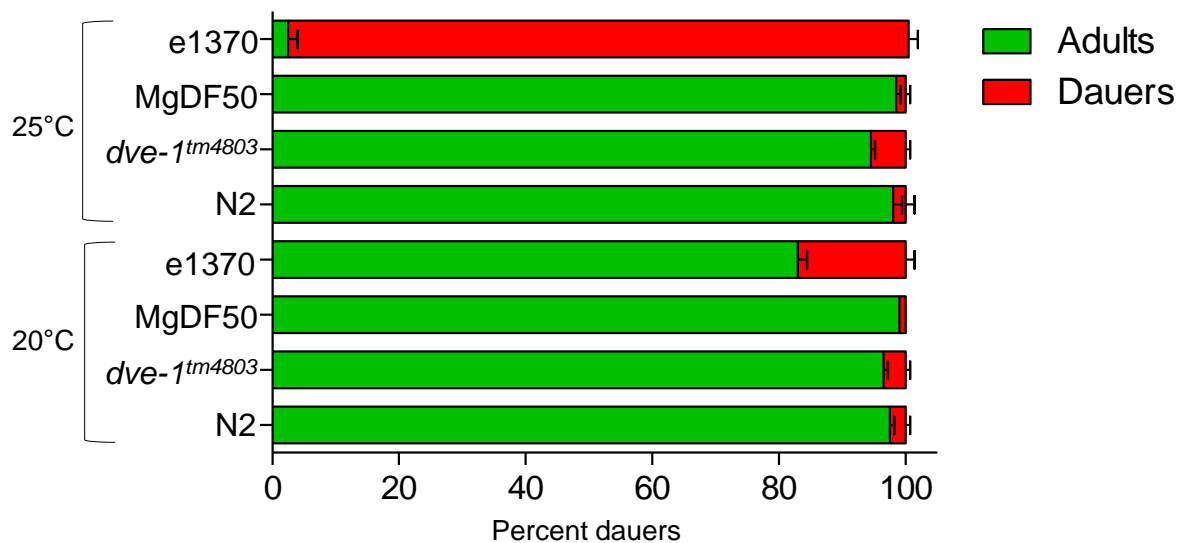


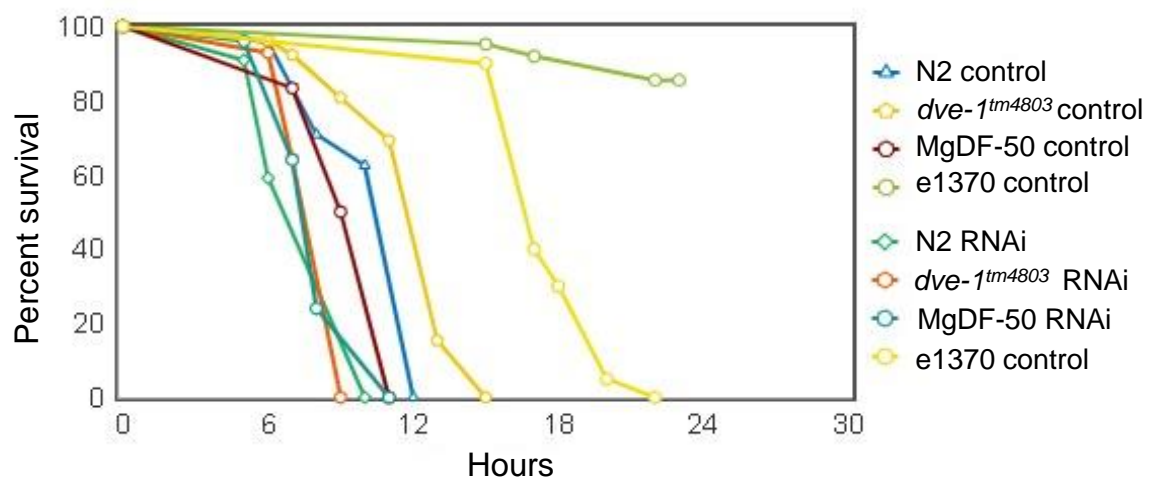
**Figure 4. 5. Dauer formation assay.**

*e1370* (*daf-2*) worms formed 100% dauers at 25°C compared to only 20% at 20°C. For other strains including *dve-1<sup>tm4803</sup>*, only a small fraction of worms became dauers even at 25°C.

#### 4.2.4 Effect of *dve-1* RNAi on stress resilience of worms

As deficiency of DVE-1 leads to a decreased lifespan, we wanted to investigate if this would also decrease the resilience of the worms under the stress conditions. We knocked down *dve-1* by feeding the dsRNA expressing bacteria and performed the oxidative and thermal stress assays again. The control RNAi showed a similar profile as before with *dve-1<sup>tm4803</sup>* outliving the wild type and the *daf-16* null strain in both oxidative and thermal stress conditions. But, upon *dve-1* KD, the resilience of *dve-1<sup>tm4803</sup>* worms to the oxidative stress reduced to that of worms of other strains.

A



B

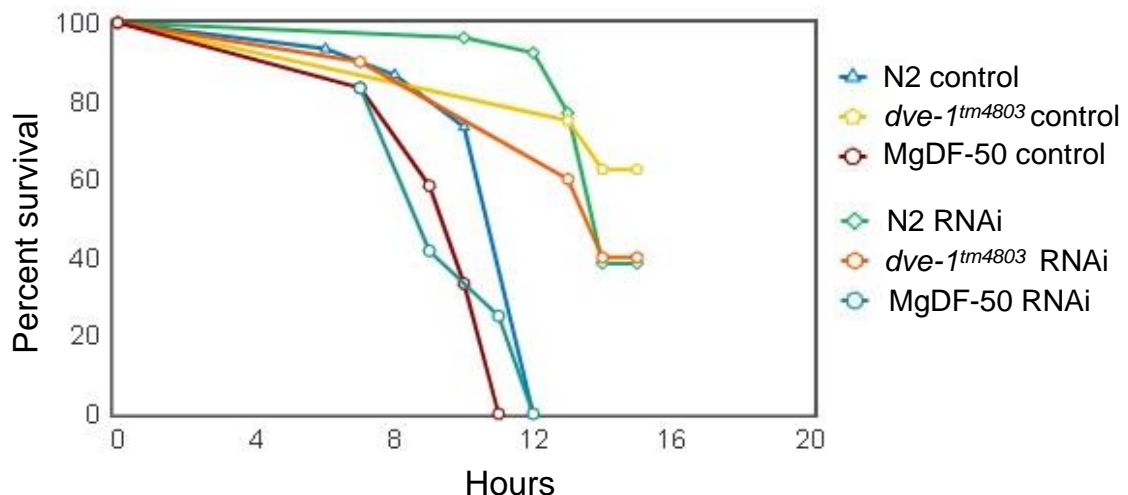


**Figure 4. 6. Stress assay upon knockdown of *dve-1*.**

The worms grown on *dve-1* RNAi plate or control RNAi plate was assayed in the Day1 adult stage. (A) *dve-1* RNAi significantly reduced the oxidative stress tolerance of worms of all the strains. (B) Upon temperature stress, *dve-1* didn't further reduce the survivability of mgDf50 or *dve-1<sup>tm4803</sup>* but that of wildtype N2 worms increased. P-value <0.0001 (Mantel-cox test).

Even for the *daf-2* (e1370) mutant, the oxidative stress tolerance decreased significantly. In the thermal stress assay, there was no effect of *dve-1* KD on the survivability of *dve-1<sup>tm4803</sup>* and the short-lived mutant, mgDf50. Surprisingly, KD of *dve-1* increased the tolerance of N2 worms to an extent similar to that of *dve-1<sup>tm4803</sup>*.

#### 4.2.5 Transcriptome analysis of *dve-1<sup>tm4803</sup>* worms reveals differential gene expression in multiple pathways

To get a better understanding of the observed phenotypes of *dve-1<sup>tm4803</sup>*, we took a genome-wide approach to dissect out the genes which were differentially regulated in *dve-1<sup>tm4803</sup>*. We performed RNA sequencing of *dve-1<sup>tm4803</sup>* in the day 1 stage of the worms and normalized the expression level of genes with that in N2 worms. We found multiple genes that had significant differential expression (Fig. 4.7). We performed the Gene-ontology (GO) analysis to dissect-out the pathways to which these genes were associated with. Most of these differentially regulated genes belonged to the pathways which were associated with the metabolism of the cell. Ageing was also one of the pathways in the GO-term analysis (Fig. 4.8).

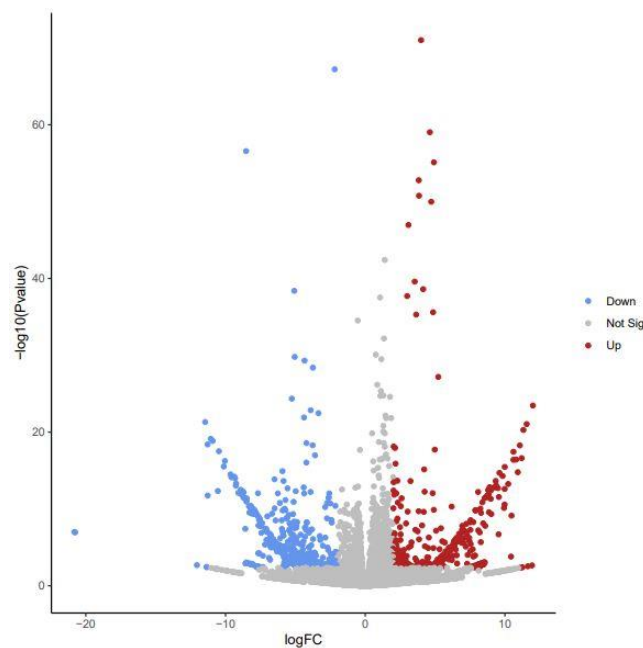


**Figure 4. 7. Volcano plot of the differentially-regulated genes.**

The volcano plot shows that large number of genes were differentially regulated in *dve-1<sup>tm4803</sup>*. 1094 transcripts were downregulated while 952 transcripts were upregulated significantly. (P-value < 0.05)

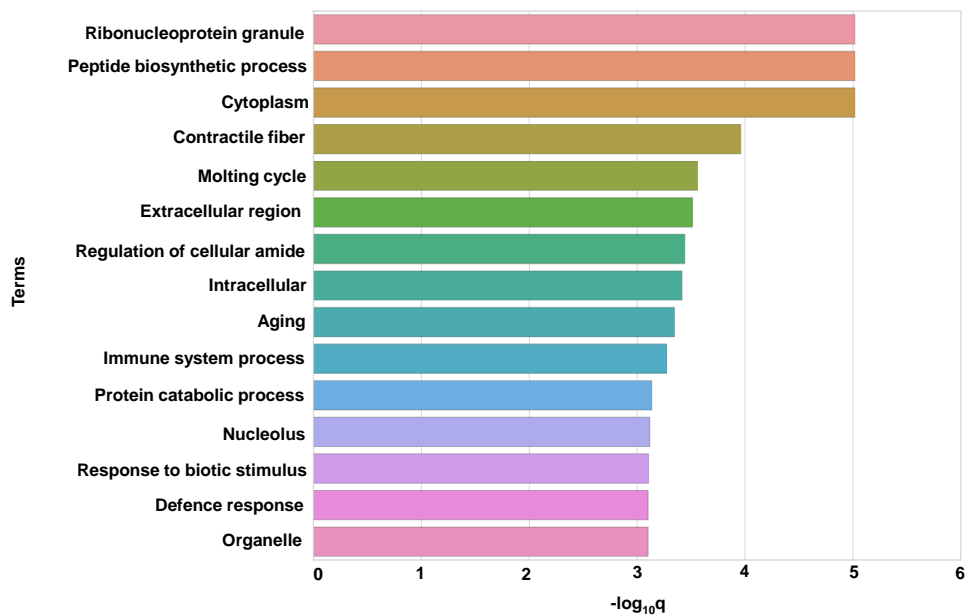


**Figure 4. 8. GO-term analysis of differentially expressed genes.**

The differentially regulated gene set was used for the Gene-ontology analysis. These genes belonged to various previously characterized biological pathways. Ageing was one of the pathways that was found. The threshold of q-value was less than 0.1.

#### 4.2.6 GO-term analysis of upregulated genes explained the thermal resilience of *dve-1<sup>tm4803</sup>*

Further, from the gene list of all differentially regulated genes, we separated the upregulated genes ( $\log_2FC > 2$ ) with  $p < 0.05$  and performed the GO-term analysis. Interestingly, we observed a set of genes that belonged to the IRE-1 mediated stress response which included the genes coding for the cytoplasmic chaperones like *hsp-16.11*, *hsp-16.2*, *hsp-70*, etc. (Fig. 4.9). The expression of these genes is known to be upregulated under the thermal stress by the binding of TF, HSF-1 on their promoters (Parsell and Lindquist, 1993; Westerheide and Morimoto, 2005). While the expression level of *hsf-1* itself didn't change significantly but the expression levels of its targets were significantly high. We verified this by qRT-PCR and the expression level of *hsp-16.11* correlated with that obtained from the RNA-sequencing. This explained the high thermal resilience of these worms compared to others. We didn't find any change in the expression level of genes coding for the chaperones associated with other organelles like *hsp-4* for ER and *hsp-6* and *hsp-60* for mitochondria.

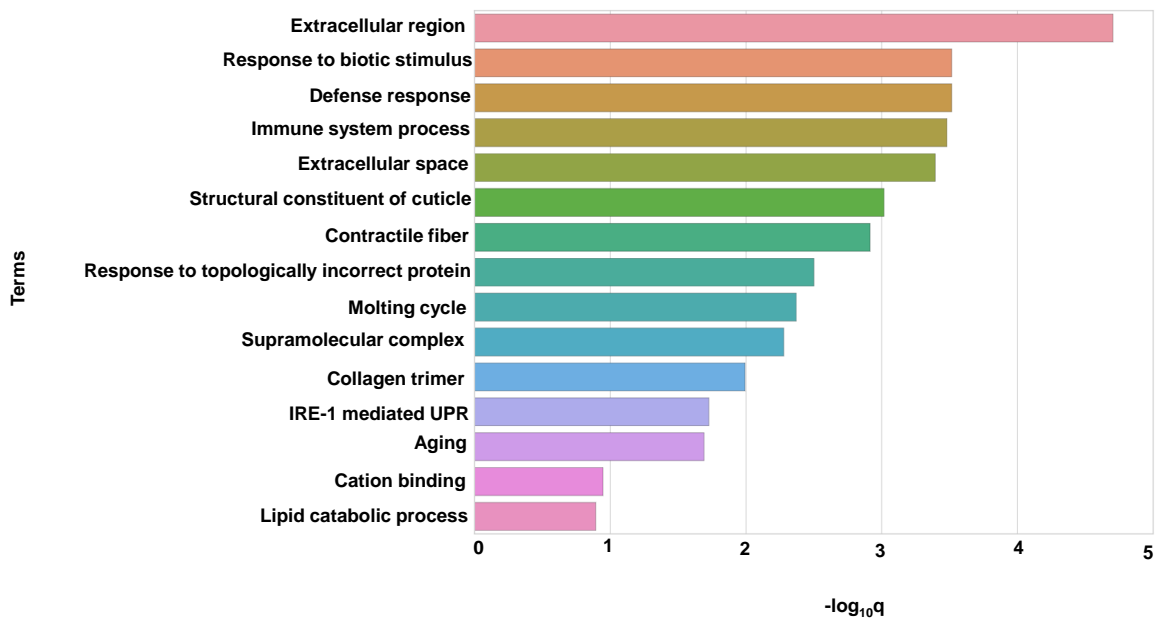


**Figure 4. 9. GO-term analysis of upregulated genes.**

The GO-term analysis of upregulated genes indicated the ageing and IRE-1 mediated UPR among prominent pathways that were upregulated. The second biological pathway contained set of cytoplasmic chaperone genes that were highly upregulated. These chaperones are thermal stress response factors.

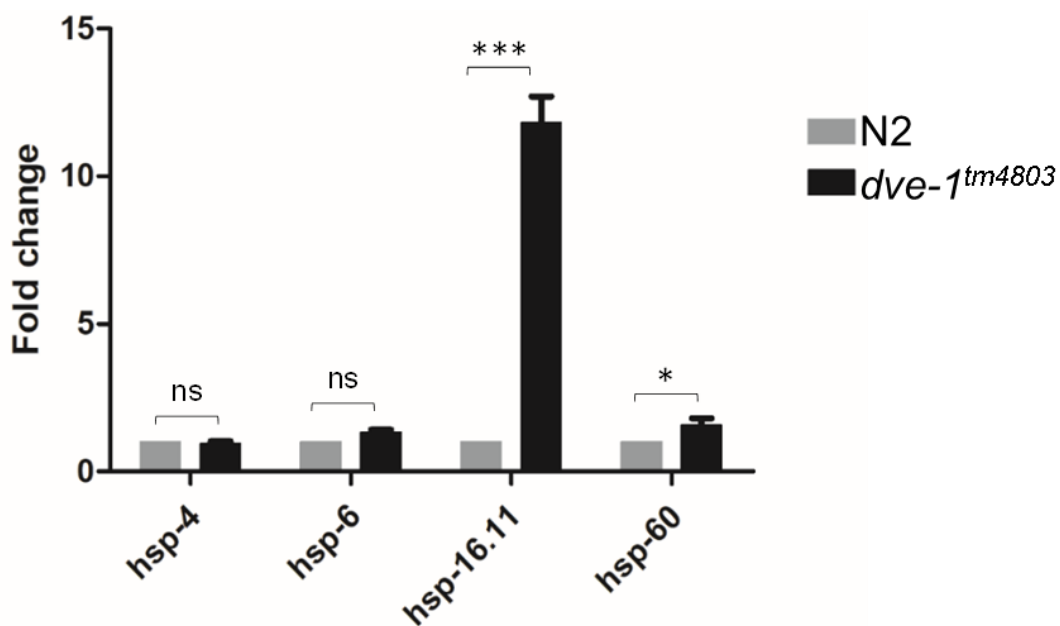


**Figure 4. 10. Expression level of chaperones of different sub-cellular compartment.**

q-PCR was performed to verify the expression level of chaperone genes in *dve-1<sup>tm4803</sup>* and N2. Expression of *hsp-4* and *hsp-6* was same in both the strains. *hsp-60* was slightly while *hsp-16.11* was highly upregulated in *dve-1<sup>tm4803</sup>*.

### 4.3 Discussion and future directions

In this study, we have attempted to investigate a novel paradigm of longevity. DVE-1 is a crucial protein in *C. elegans* for development, stress response, and lifespan (Haynes et al., 2007). It has been best studied for its role in relaying the information of protein misfolding from mitochondria to nucleus along with ATFS-1 and UBL-5 (Haynes et al., 2007; Durieux et al., 2011). The deficiency of any of these proteins decreases the lifespan of the worms due to the inability of worms to upregulate the expression of protective chaperones in stress. On the other hand, RNAi of genes coding for the components of the mitochondrial electron transport system like *cco-1*, *nuo-6*, *isp-1*, *clk-1*, etc. increases the lifespan due to the hormetic stress which leads to the increased basal expression of *hsp-6* and *hsp-60* (Wu et al., 2018). But not all genes that lead to UPR<sup>mt</sup> confer longevity upon knockdown, indicative of the insufficiency of UPR<sup>mt</sup> to increase the lifespan of the organisms. Besides, KD of *cco-1* increases the lifespan even in the deficiency of ATFS-1 that prevents UPR<sup>mt</sup> (Bennett et al., 2014). But in any background, *dve-1* KD decreases the lifespan of worms which meant it might serve unexplored critical functions in cells other than activation of UPR<sup>mt</sup>.

We found a long-lived *dve-1<sup>tm4803</sup>* mutant that contained a deletion in the gene body of *dve-1*. This mutation conferred high-stress tolerance to these worms like the other long-lived mutants. The KD of *dve-1* in *dve-1<sup>tm4803</sup>* decreased the oxidative stress tolerance of the worms while the thermal tolerance remained largely unaffected. This meant the genes associated with the heat-shock response were constitutively upregulated and might not have affected even upon the KD of *dve-1*. This mutation in *dve-1* might have led to the upregulation of these HSPs as a compensatory mechanism which has also been the case of other mitochondrial mutants (Labbadia et al., 2017). But this doesn't explain the increased oxidative stress response which sharply diminished by the *dve-1* RNAi. One possibility is that the truncated DVE-1<sup>tm4803</sup> could have some gain-of-function which might have conferred at least a part of the observed phenotype. DVE-1 remains cytoplasmic due to the SUMOylation at K327 residue under the normal condition. Only in the mitochondrial stress, ULP-4 de-SUMOylates DVE-1 which then undergoes nuclear accumulation (Gao et al., 2019). The deletion in *dve-1<sup>tm4803</sup>* spans this region of protein and DVE-1<sup>tm4803</sup> was found to

be in the nuclear fraction. DVE-1<sup>tm4803</sup> in the nucleus could bind to the target genes and modulate their expression level even under the normal condition.

Further investigations are required to understand the underlying mechanism of longevity. We plan to use RNAi of the genes which were found to be differentially regulated in *dve-1<sup>tm4803</sup>* to find the downstream targets of DVE-1. Also, with the genetic manipulations, we wish to study the putative role of DAF-16 in this system.



## References

- Antebi A, Norris CR, Hedgecock EM, et al. Cell and Growth Cone Migrations. In: Riddle DL, Blumenthal T, Meyer BJ, et al., editors. *C. elegans* II. 2nd edition. Cold Spring Harbor (NY): Cold Spring Harbor Laboratory Press; 1997. Chapter 21.
- Cassada, R.C. and Russell, R.L. 1975. The dauer larva, a postembryonic developmental variant of the nematode *Caenorhabditis elegans*. *Dev. Biol.* **46**: 326-342.
- Agrelo, R., Souabni, A., Novatchkova, M., Haslinger, C., Komnenovic, V., Kishimoto, H., Gresh, L., Kohwi-, T., Kenner, L., and Wutz, A. (2014). NIH Public Access. *16*, 507–516.
- Bennett, C.F., Vander Wende, H., Simko, M., Klum, S., Barfield, S., Choi, H., Pineda, V. V, and Kaeberlein, M. (2014). Activation of the mitochondrial unfolded protein response does not predict longevity in *Caenorhabditis elegans*. *Nat. Commun.* **5**, 3483.
- Berdichevsky, A., Viswanathan, M., Horvitz, H.R., and Guarente, L. (2006). with 14-3-3 Proteins to Activate DAF-16 and Extend Life Span. 1165–1177.
- Bertolotti, A., Zhang, Y., Hendershot, L.M., Harding, H.P., and Ron, D. (2000). Dynamic interaction of BiP and ER stress transducers in the unfolded-protein response. *Nat. Cell Biol.* **2**, 326–332.
- Cantrell, D.A. (2001). Phosphoinositide 3-kinase signalling pathways. *J. Cell Sci.* **114**, 1439 LP-1445.
- Ceron, J., Ceron, J., Koreth, J., Koreth, J., Hao, T., Hao, T., Nicot, A., Nicot, A., Hirozane-kishikawa, T., Hirozane-kishikawa, T., et al. (2004). Toward Improving. *Genome Res.* 2162–2168.
- Chapman, T., and Partridge, L. (1996). Female fitness in *Drosophila melanogaster*: An interaction between the effect of nutrition and of encounter rate with males. *Proc. R. Soc. B Biol. Sci.* **263**, 755–759.
- Cohen, E., Du, D., Joyce, D., Kapernick, E.A., Volovik, Y., Kelly, J.W., and Dillin, A.

(2010). Temporal requirements of insulin/IGF-1 signaling for proteotoxicity protection. *Aging Cell* 9, 126–134.

Davidovic, M., Sevo, G., Svorcan, P., Milosevic, D.P., Despotovic, N., and Erceg, P. (2010). Old age as a privilege of the “selfish ones.” *Aging Dis.* 1, 139–146.

Drechsel, D.A., and Patel, M. (2008). Free Radical Biology & Medicine Role of reactive oxygen species in the neurotoxicity of environmental agents implicated in Parkinson ' s disease. 44, 1873–1886.

Durieux, J., Wolff, S., and Dillin, A. (2011). The Cell-Non-Autonomous Nature of Electron Transport Chain-Mediated Longevity. *Cell* 144, 79–91.

Ellis, R.J. (2001). Macromolecular crowding: Obvious but underappreciated. *Trends Biochem. Sci.* 26, 597–604.

Faber, P.W., Alter, J.R., Macdonald, M.E., and Hart, A.C. (1999). Polyglutamine-mediated dysfunction and apoptotic death of a *Caenorhabditis elegans* sensory neuron. *Proc. Natl. Acad. Sci. U. S. A.* 96, 179–184.

Francisco, S., and Ranch, T.S. (1998). HOW AND WHY WE AGE. 33, 639–653.

Gao, K., Li, Y., Hu, S., and Liu, Y. (2019). SUMO peptidase ULP-4 regulates mitochondrial UPR-mediated innate immunity and lifespan extension. 1–24.

Gems, D., Sutton, A.J., Sundermeyer, M.L., Albert, P.S., King, K. V, Edgley, M.L., Larsen, P.L., and Riddle, D.L. (1998). Two Pleiotropic Classes of *daf-2* Mutation Affect Larval Arrest, Adult Behavior, Reproduction and Longevity in *Caenorhabditis elegans*; *Genetics* 150, 129 LP-155.

Gerisch, B., Weitzel, C., Kober-Eisermann, C., Rottiers, V., and Antebi, A. (2001). A Hormonal Signaling Pathway Influencing *C. elegans* Metabolism, Reproductive Development, and Life Span. *Dev. Cell* 1, 841–851.

Gerschman, R., Gilbert, D.L., Nye, S.W., Dwyer, P., and Fenn, W.O. (1954). Oxygen Poisoning and X-irradiation: A Mechanism in Common. *Science* (80- ). 119, 623 LP-626.

Gottimukkala, K.P., Burute, M., and Galande, S. (2012). SATB1: Key Regulator of T Cell Development and Differentiation. In *Hematology*, C.H. Lawrie, ed. (Rijeka:

IntechOpen), p.

Gottlieb, S., and Ruvkun, G. (1994a). *daf-2*, *daf-16* and *daf-23*: Genetically interacting genes controlling dauer formation in *Caenorhabditis elegans*. *Genetics* 137, 107–120.

Gottlieb, S., and Ruvkun, G. (1994b). *daf-2*, *daf-16* and *daf-23*: genetically interacting genes controlling Dauer formation in *Caenorhabditis elegans*. *Genetics* 137, 107–120.

Gredilla, R., and Barja, G. (2005). Minireview : The Role of Oxidative Stress in Relation to Caloric Restriction and Longevity. 146, 3713–3717.

Harris, T.W., Chen, N., Cunningham, F., Tello-Ruiz, M., Antoshechkin, I., Bastiani, C., Bieri, T., Blasiar, D., Bradnam, K., Chan, J., et al. (2004). WormBase: a multi-species resource for nematode biology and genomics. *Nucleic Acids Res.* 32, D411–D417.

Hassan, M., and Abedi-Valugerdi, M. (2014). Hematologic malignancies in elderly patients. *Haematologica* 99, 1124–1127.

Hayflick, L. (1965). The limited in vitro lifetime of human diploid cell strains. *Exp. Cell Res.* 37, 614–636.

Haynes, C.M., Petrova, K., Benedetti, C., Yang, Y., and Ron, D. (2007). ClpP Mediates Activation of a Mitochondrial Unfolded Protein Response in *C. elegans*. *Dev. Cell* 13, 467–480.

van Heemst, D. (2010). Insulin, IGF-1 and longevity. *Aging Dis.* 1, 147–157.

Hiyama, E., and Hiyama, K. (2007). Telomere and telomerase in stem cells. *Br. J. Cancer* 96, 1020–1024.

Hsu, A.L., Murphy, C.T., and Kenyon, C. (2003). Regulation of aging and age-related disease by DAF-16 and heat-shock factor. *Science* (80- ). 300, 1142–1145.

Ikenaka, K., Tsukada, Y., Giles, A.C., Arai, T., Nakadera, Y., Nakano, S., Kawai, K., Mochizuki, H., Katsuno, M., Sobue, G., et al. (2019). A behavior-based drug screening system using a *Caenorhabditis elegans* model of motor neuron disease. *Sci. Rep.* 9, 1–10.

Johnston, R.J., Otake, Y., Sood, P., Vogt, N., Behnia, R., Vasiliauskas, D., McDonald, E., Xie, B., Koenig, S., Wolf, R., et al. (2011). Interlocked feedforward loops control cell-type-specific rhodopsin expression in the drosophila eye. *Cell* 145, 956–968.

Kamath, R.S., and Ahringer, J. (2003). Genome-wide RNAi screening in *Caenorhabditis elegans*. *Methods* 30, 313–321.

Keane, P.C., Kurzawa, M., Blain, P.G., and Morris, C.M. (2011). Mitochondrial Dysfunction in Parkinson's Disease. *Park. Dis.* 2011, 716871.

Kenyon, C.J. (2010). The genetics of ageing. *Nature* 464, 504–512.

Khare, S.P., Shetty, A., Biradar, R., Patta, I., Chen, Z.J., Sathe, A. V, Reddy, P.C., Lahesmaa, R., and Galande, S. (2019). NF- $\kappa$ B Signaling and IL-4 Signaling Regulate SATB1 Expression via Alternative Promoter Usage During Th2 Differentiation. *Front. Immunol.* 10, 667.

Kimura, K.D., Tissenbaum, H.A., Liu, Y., and Ruvkun, G. *daf-2*, an Insulin Receptor – Like Gene That Regulates Longevity and Diapause in *Caenorhabditis elegans*.

Kirkwood, T.B.L., and Cremer, T. (1982). Cyto gerontology since 1881: A reappraisal of August Weismann and a review of modern progress. *Hum. Genet.* 60, 101–121.

Klass, M.R. (1977). Aging in the nematode *Caenorhabditis elegans*: Major biological and environmental factors influencing life span. *Mech. Ageing Dev.* 6, 413–429.

Kondo, M., Senoo-Matsuda, N., Yanase, S., Ishii, T., Hartman, P.S., and Ishii, N. (2005). Effect of oxidative stress on translocation of DAF-16 in oxygen-sensitive mutants, *mev-1* and *gas-1* of *Caenorhabditis elegans*. *Mech. Ageing Dev.* 126, 637–641.

Kudron, M.M., Victorsen, A., Gevirtzman, L., Hillier, L.W., Fisher, W.W., Vafeados, D., Kirkey, M., Hammonds, A.S., Gersch, J., Ammouri, H., et al. (2018). The ModERN Resource: Genome-Wide Binding Profiles for Hundreds of *Drosophila* and *Caenorhabditis elegans* Transcription Factors. 208, 937–949.

Labbadia, J., Brielmann, R.M., Neto, M.F., Lin, Y.-F., Haynes, C.M., and Morimoto, R.I. (2017). Mitochondrial Stress Restores the Heat Shock Response and Prevents Proteostasis Collapse during Aging. *Cell Rep.* 21, 1481–1494.

Lakso, M., Vartiainen, S., Moilanen, A.M., Sirviö, J., Thomas, J.H., Nass, R., Blakely, R.D., and Wong, G. (2003). Dopaminergic neuronal loss and motor deficits in *Caenorhabditis elegans* overexpressing human  $\alpha$ -synuclein. *J. Neurochem.* 86, 165–172.

- Lee, S.S., Kennedy, S., Tolonen, A.C., and Ruvkun, G. (2003). DAF-16 target genes that control *C. elegans* Life-span and metabolism. *Science* (80- ). 300, 644–647.
- Lin, X.-X., Sen, I., Janssens, G.E., Zhou, X., Fonslow, B.R., Edgar, D., Stroustrup, N., Swoboda, P., Yates, J.R., Ruvkun, G., et al. (2018). DAF-16/FOXO and HLH-30/TFEB function as combinatorial transcription factors to promote stress resistance and longevity. *Nat. Commun.* 9, 4400.
- Link, C.D. (1995). Expression of human  $\beta$ -amyloid peptide in transgenic *Caenorhabditis elegans*. *Proc. Natl. Acad. Sci. U. S. A.* 92, 9368–9372.
- Liou, G.-Y., and Storz, P. (2010). Reactive oxygen species in cancer. *Free Radic. Res.* 44, 479–496.
- Luo, R.Z.-T., Beniac, D.R., Fernandes, A., Yip, C.C., and Ottensmeyer, F.P. (1999). Quaternary Structure of the Insulin-Insulin Receptor Complex. *Science* (80- ). 285, 1077 LP-1080.
- Manuscript, A. (2009). *NIH Public Access.* 3, 698–709.
- Maras, J.E., Talegawkar, S.A., Qiao, N., Lyle, B., Ferrucci, L., and Tucker, K.L. (2011). Flavonoid intakes in the Baltimore Longitudinal Study of Aging. *J. Food Compos. Anal.* 24, 1103–1109.
- Mata-Cabana, A., Sin, O., Seinstra, R.I., and Nollen, E.A.A. (2018). Nuclear/Cytoplasmic Fractionation of Proteins from *Caenorhabditis elegans*. *Bio-Protocol* 8, e3053.
- Mayer, M.P., and Bukau, B. (2005). Hsp70 chaperones: Cellular functions and molecular mechanism. *Cell. Mol. Life Sci.* 62, 670–684.
- McCay, C.M., Crowell, M.F., and Maynard, L.A. (1935). The Effect of Retarded Growth Upon the Length of Life Span and Upon the Ultimate Body Size: One Figure. *J. Nutr.* 10, 63–79.
- Minami, R., Wakabayashi, M., Sugimori, S., Taniguchi, K., Kokuryo, A., Imano, T., Adachi-Yamada, T., Watanabe, N., and Nakagoshi, H. (2012). The homeodomain protein defective proventriculus is essential for male accessory gland development to enhance fecundity in *Drosophila*. *PLoS One* 7.

- Mir, R., Pradhan, S.J., and Galande, S. (2012). Chromatin organizer SATB1 as a novel molecular target for cancer therapy. *Curr. Drug Targets* 13, 1603–1615.
- Mishra, P., and Chan, D.C. (2014). Mitochondrial dynamics and inheritance during cell division, development and disease. *Nat. Rev. Mol. Cell Biol.* 15, 634–646.
- Moreira, P.I., Carvalho, C., Zhu, X., Smith, M.A., and Perry, G. (2010). Mitochondrial dysfunction is a trigger of Alzheimer's disease pathophysiology. *Biochim. Biophys. Acta - Mol. Basis Dis.* 1802, 2–10.
- Muschiol, D., Schroeder, F., and Traunspurger, W. (2009). Life cycle and population growth rate of *Caenorhabditis elegans* studied by a new method. *BMC Ecol.* 9, 14.
- Nakagawa, Y., Fujiwara-Fukuta, S., Yorimitsu, T., Tanaka, S., Minami, R., Shimooka, L., and Nakagoshi, H. (2011). Spatial and temporal requirement of Defective proventriculus activity during *Drosophila* midgut development. *Mech. Dev.* 128, 258–267.
- Nargund, A.M., Pellegrino, M.W., Fiorese, C.J., Baker, B.M., and Haynes, C.M. (2012). Mitochondrial Import Efficiency of ATFS-1 Regulates Mitochondrial UPR Activation. *Science* (80-. ). 337, 587 LP-590.
- Nechanitzky, R., Dávila, A., Savarese, F., Fietze, S., and Grosschedl, R. (2012). *Satb1* and *Satb2* Are Dispensable for X Chromosome Inactivation in Mice. *Dev. Cell* 23, 866–871.
- O'Reilly, L.P., Luke, C.J., Perlmutter, D.H., Silverman, G.A., and Pak, S.C. (2014). *C. elegans* in high-throughput drug discovery. *Adv. Drug Deliv. Rev.* 69–70, 247–253.
- Oh, S.W., Mukhopadhyay, A., Svzrikapa, N., Jiang, F., Davis, R.J., and Tissenbaum, H.A. (2005). JNK regulates lifespan in *Caenorhabditis elegans* by modulating nuclear translocation of forkhead transcription factor/DAF-16. *Proc. Natl. Acad. Sci. U. S. A.* 102, 4494–4499.
- Parsell, D.A., and Lindquist, S. (1993). THE FUNCTION OF HEAT -SHOCK PROTEINS IN STRESS TOLERANCE : DEGRADATION AND REACTIV ATION OF DAMAGED PROTEINS. 437–496.
- Pellegrino, M.W., Nargund, A.M., and Haynes, C.M. (2013). Signaling the mitochondrial unfolded protein response. *Biochim. Biophys. Acta* 1833, 410–416.

Pierce, S.B., Costa, M., Wisotzkey, R., Devadhar, S., Homburger, S.A., Buchman, A.R., Ferguson, K.C., Heller, J., Platt, D.M., Pasquinelli, A.A., et al. (2001). Regulation of DAF-2 receptor signaling by human insulin and ins-1 , a member of the unusually large and diverse *C. elegans* insulin gene family. 672–686.

Pratt, W.B., and Toft, D.O. (2003). Regulation of Signaling Protein Function and Trafficking by the hsp90/hsp70-Based Chaperone Machinery. *Exp. Biol. Med.* 228, 111–133.

Rätsch, G., Sonnenburg, S., Srinivasan, J., Witte, H., Müller, K.-R., Sommer, R.-J., and Schölkopf, B. (2007). Improving the *Caenorhabditis elegans* genome annotation using machine learning. *PLoS Comput. Biol.* 3, e20–e20.

Ruben, A.J., and Biology, E. (2000). Hayflick , his limit , and cellular ageing. 1, 72–76.

Savarese, F., Dávila, A., Nechanitzky, R., De La Rosa-Velazquez, I., Pereira, C.F., Engelke, R., Takahashi, K., Jenuwein, T., Kohwi-Shigematsu, T., Fisher, A.G., et al. (2009). Satb1 and Satb2 regulate embryonic stem cell differentiation and Nanog expression. *Genes Dev.* 23, 2625–2638.

Scheuner, D., Song, B., McEwen, E., Liu, C., Laybutt, R., Gillespie, P., Saunders, T., Bonner-Weir, S., and Kaufman, R.J. (2001). Translational control is required for the unfolded protein response and in vivo glucose homeostasis. *Mol. Cell* 7, 1165–1176.

Sharma, P., Jha, A.B., Dubey, R.S., and Pessaraki, M. (2012). Reactive Oxygen Species, Oxidative Damage, and Antioxidative Defense Mechanism in Plants under Stressful Conditions. *J. Bot.* 2012, 217037.

Shen, X., Ellis, R.E., Lee, K., Liu, C.Y., Yang, K., Solomon, A., Yoshida, H., Morimoto, R., Kurnit, D.M., Mori, K., et al. (2001). Complementary signaling pathways regulate the unfolded protein response and are required for *C. elegans* development. *Cell* 107, 893–903.

Tepper, R.G., Ashraf, J., Kaletsky, R., Kleemann, G., Murphy, C.T., and Bussemaker, H.J. (2013). PQM-1 complements DAF-16 as a key transcriptional regulator of DAF-2-mediated development and longevity. *Cell* 154, 676–690.

Volovik, Y., Moll, L., Marques, F.C., Maman, M., Bejerano-Sagie, M., and Cohen, E. (2014). Differential Regulation of the Heat Shock Factor 1 and DAF-16 by Neuronal

nhl-1 in the Nematode *C.elegans*. *Cell Rep.* 9, 2192–2205.

Wang, Q., Qian, J., Wang, F., and Ma, Z. (2012). Cellular prion protein accelerates colorectal cancer metastasis via the Fyn-SP1-SATB1 axis. *Oncol. Rep.* 28, 2029–2034.

Westerheide, S.D., and Morimoto, R.I. (2005). Heat Shock Response Modulators as Therapeutic Tools for Diseases of Protein Conformation. *J. Biol. Chem.* 280, 33097–33100.

Wu, Z., Senchuk, M.M., Dues, D.J., Johnson, B.K., Cooper, J.F., Lew, L., Machiela, E., Schaar, C.E., DeJonge, H., Blackwell, T.K., et al. (2018). Mitochondrial unfolded protein response transcription factor ATFS-1 promotes longevity in a long-lived mitochondrial mutant through activation of stress response pathways. *BMC Biol.* 16, 1–19.

Zweegman, S., Palumbo, A., Bringhen, S., and Sonneveld, P. (2014). Age and aging in blood disorders: multiple myeloma. *Haematologica* 99, 1133–1137.

Sulston, J. E., Schierenberg, E., White, J. G., & Thomson, J. N. (1983). The embryonic cell lineage of the nematode *Caenorhabditis elegans*. *Developmental Biology*, 100(1), 64–119. doi:10.1016/0012-1606(83)90201-4



## Appendix: Raw data for phenotypic assays

**Table 1. Lifespan assay of N2 and *dve-1<sup>tm4803</sup>***

	N2	<i>dve-1<sup>tm4803</sup></i>
# of blank lines	70	106
# rows with impossible data	0	0
# censored subjects	9	11
# deaths/events	106	70
Median survival (Days)	15	21

**Table 2. Temperature stress assay**

	<i>dve-1<sup>tm4803</sup></i> (35°C)	<i>mgDF50</i> (35°C)	<i>dve-1<sup>tm4803</sup></i> (20°C)	<i>mgDF50</i> (20°C)	N2 (35°C)	N2 (20°C)
Number of rows	344	344	344	344	344	344
# of blank lines	220	219	343	343	254	343
# rows with impossible data	0	0	0	0	0	0
# censored subjects	4	5	1	1	6	1
# deaths/events	124	125	0	0	120	0
Median survival	15	9	Undefined	Undefined	10	Undefined

**Table 3. TBHP stress assay**

	<i>dve-1<sup>tm4803</sup></i>	<i>mgdf-50</i>	N2	N2 (Control)	<i>mgDF50</i> (Control)	<i>dve-1<sup>tm4803</sup></i> (Control)
Number of rows	273	273	273	273	273	273
# of blank lines	126	205	218	272	272	272
# rows with impossible data	0	0	0	0	0	0
# censored subjects	6	2	8	1	1	1
# deaths/events	147	145	153	0	0	0
Median survival	8	6	6	Undefined	Undefined	Undefined

**Table 4. Dauer formation assay**

Temperature (°C)	Strain name	Adults			Dauers		
		Mean	SD	Replicates	Mean	SD	Replicates
20	N2	97.5	0.7	2	2.5	0.7	2
20	<i>dve-1<sup>tm4803</sup></i>	96.5	0.7	2	3.5	0.7	2
20	mgDf50	99	0	2	1	0	2
20	e1370	83	1.41	2	17	1.41	2
25	N2	98	1.41	2	2	1.41	2
25	<i>dve-1<sup>tm4803</sup></i>	94.5	0.7	2	5.5	0.7	2
25	mgDf50	98.5	0.7	2	1.5	0.7	2
25	e1370	2.5	1.414	2	98	1.414	2

